ELECTROCHEMICAL PRODUCTION OF TUNGSTEN REFRACTORY METAL POWDERS

A THESIS SUBMITTED TO
THE GRADUATE SCHOOL OF NATURAL AND APPLIED SCIENCES
OF
MIDDLE EAST TECHNICAL UNIVERSITY

BY

FURKAN ÖZDEMİR

IN PARTIAL FULFILLMENT OF THE REQUIREMENTS
FOR
THE DEGREE OF MASTER OF SCIENCE
IN
METALLURGICAL AND MATERIALS ENGINEERING

FEBRUARY 2017

Approval of the thesis:

ELECTROCHEMICAL PRODUCTION OF TUNGSTEN REFRACTORY METAL POWDERS

submitted by **FURKAN ÖZDEMİR** in partial fulfillment of the requirements for the degree of **Master of Science in Metallurgical and Materials Engineering Department, Middle East Technical University** by,

Prof. Dr. Gülbin Dural Ünver _____
Dean, Graduate School of **Natural and Applied Science**

Prof. Dr. Cemil Hakan Gür _____
Head of Department, **Metallurgical and Materials Engineering**

Prof. Dr. İshak Karakaya _____
Supervisor, **Metallurgical and Materials Eng. Dept., METU**

Assist. Prof. Dr. Metehan Erdoğan _____
Co-Supervisor, **Materials Engineering Dept., AYBU**

Examining Committee Members:

Prof. Dr. Kadri Aydınol _____
Metallurgical and Materials Engineering Dept., METU

Prof. Dr. İshak Karakaya _____
Metallurgical and Materials Engineering Dept., METU

Assist. Prof. Dr. Metehan Erdoğan _____
Materials Engineering Dept., AYBU

Assist. Prof. Dr. Erkan Konca _____
Metallurgical and Materials Engineering Dept., Atılım University

Assist. Prof. Dr. Batur Ercan _____
Metallurgical and Materials Engineering Dept., METU

Date: 03/02/2017

I hereby declare that all information in this document has been obtained and presented in accordance with academic rules and ethical conduct. I also declare that, as required by these rules and conduct, I have fully cited and referenced all material and results that are not original to this work.

Name, Last name: FURKAN ÖZDEMİR

Signature :

ABSTRACT

ELECTROCHEMICAL PRODUCTION OF TUNGSTEN REFRACTORY METAL POWDERS

Özdemir, Furkan
M.S., Department of Metallurgical and Materials Engineering
Supervisor: Prof. Dr. İshak Karakaya
Co-supervisor: Assist. Prof. Dr. Metehan Erdoğan
February 2017, 72 pages

Tungsten is mainly produced by H_2 reduction of WO_3 which makes its production difficult and costly. A promising method was recently reported for direct electrochemical production of tungsten from $CaWO_4$ (scheelite) which is estimated as the seventy percent of the all tungsten reserves of the world. This thesis investigated the possible improvements that could be made on the direct electrochemical reduction method mentioned above. In this study, the experiments were divided into two sections, namely laboratory and large scale experiments.

In the laboratory scale experiments, the application of pulse current was studied in the electrochemical reduction of 2.5 grams of $CaWO_4$ pellets attached to a current collector. The electrolyte was composed of calcium chloride and sodium chloride salts at eutectic composition (48 pct mol NaCl at 873 K). The reduced samples were cleaned with dilute hydrochloric acid solutions and characterized by X-ray diffraction and scanning electron microscopy. Examination of the results revealed that metallic tungsten was obtained by pulse current reduction. Analysis of the results

indicated that pulse current application was more energy efficient than the constant current studies. Also, the final shapes of product powders varied with the pulse parameters.

In the large scale experiments, a pilot tungsten production system with a production capacity of 60-100 grams of tungsten per batch was designed and modified to approach industrial scale production. The constant voltage was applied to $CaWO_4$ which was in a similar electrolytic condition as the laboratory scale experiments. The biggest problem in the large scale was the incomplete reduction. The modifications in the cell vessel and the graphite electrode significantly increased the amount of reduction.

Keywords: Electrodeoxidation, Tungsten, Scheelite, $CaWO_4$, Pulse Current, Molten Salt Electrolysis

ÖZ

TUNGSTEN REFRAKTER METAL TOZLARININ ELEKTROKİMYASAL ÜRETİMİ

Özdemir, Furkan
Yüksek Lisans, Metalurji ve Malzeme Mühendisliği Bölümü
Tez Yöneticisi: Prof. Dr. İshak Karakaya
Ortak Tez Yöneticisi: Yrd. Doç. Dr. Metehan Erdoğan
Şubat 2017, 72 sayfa

Tungsten, başlıca üretimi zor ve maliyetli bir yol olan WO_3'in H_2 ile indirgenmesinden elde edilir. Yakın bir zaman önce, dünya tungsten rezervlerinin yaklaşık yüzde yetmişini oluşturan $CaWO_4$'ın elektrokimyasal yöntemlerle doğrudan indirgenmesini içeren umut vaat edici bir tungsten üretim tekniği geliştirilmiştir Bu tezde, yukarıda bahsedilen doğrudan elektrokimyasal üretim yöntemini daha da ileriye taşımaya yönelik çalışmalar yapılmıştır. Yapılan çalışmalar, laboratuvar ölçekli ve büyük ölçekli deneyler olmak üzere iki başlıkta toplanmıştır.

Laboratuvar ölçekli çalışmalarda, bir akım toplayıcısına yerleştirilmiş 2.5 gramlık $CaWO_4$ peletlerinin darbeli akım uygulanarak indirgenmesi çalışılmıştır. Elektrolit, ergimiş $CaCl_2$ ve NaCl tuzarının ötektik kompozisyonundan (48% mol NaCl, 873 K) oluşturulmuştur. İndirgenen numuneler seyreltik HCl çözeltisinde temizleme işlemine tabi tutulmuş ve sonrasında tarama elektron mikroskopu ve X-ışınları kırınımı ile karakterize edilmiştir. Elde edilen sonuçlar, metalik tungsten tozlarının darbeli akım uygulamasıyla elde edilebildiğini göstermiştir. Sonuçların analizi, darbeli akım uygulamasının literatürdeki sabit akım uygulamalarına göre daha enerji

tasarruflu bir yöntem olabileceğini göstermiştir. Ayrıca elde edilen ürünlerin tane şekilleri darbeli akım parametrelerine göre farklılıklar göstermiştir.

Büyük ölçekli deneylerde; endüstriyel koşullara yaklaşmak için, üretim başına 60 ile 100 gram arasında tungsten üretebilecek pilot ölçekli bir tungsten üretim sistemi tasarlanmış ve modifiye edilmiştir. Laboratuvar ölçekli elektrolite benzer bir çözeltide, $CaWO_4$'a sabit potansiyel uygulaması çalışılmıştır. Elde edilen sonuçlar indirgenmenin tamamen gerçekleşmediğini göstermiştir. Hücre kazanında ve elektrotlarda yapılan modifikasyonlar sonucunda indirgenme miktarı oldukça önemli miktarlarda arttırılmıştır.

Anahtar Kelimeler: Elektrodeoksidasyon, Darbeli akım, Tungsten, Şelit, Erimiş Tuz Elektrolizi



To my family

ACKNOWLEDGEMENTS

I would like to express my gratitude cordially to my supervisor Prof. Dr. İshak Karakaya for his patience, guidance, advice, criticism, support and insight not only throughout this thesis but in many other studies.

I also wish to express my gratitude to my co-supervisor Assist. Prof. Dr. Metehan Erdoğan for his motivation, guidance, advice, criticism, support and comments during the course of this study.

I am sincerely grateful to Prof. Dr. Kadri Aydınol, Assist. Prof. Dr. Erkan Konca, and Assist. Prof. Dr. Batur Ercan for their suggestions, comments and support. I am grateful to Salih Türe, Cemal Yanardağ, Atalay Özdemir, İshak Açiş and Nilüfer Özel for their technical assistance and suggestions.

Many thanks go to members of Thermochemical and Electrochemical Materials Processing Laboratory, especially Mustafa Serdal Aras, Rauf Aksu and Oğuzhan Daldal for their support and assistance throughout this thesis.

And last, but not least, I would like to express my deepest gratitude to my parents and brother for their unconditional and deep love, and spiritual support.

This research was funded by the SAN-TEZ (0277.STZ-2013-2) project. Therefore, I would like to acknowledge the financial support provided by the Ministry of Science, Industry and Technology of Turkey and Roketsan Incorporation.

TABLE OF CONTENTS

ABSTRACT v

ÖZ vii

ACKNOWLEDGEMENTS x

LIST OF TABLES xiii

LIST OF FIGURES xiv

CHAPTERS

1.INTRODUCTION 1

1.1 Aim of this study 3

2.LITERATURE REVIEW 5

2.1 Tungsten 5

2.2 History of Tungsten [9] 6

2.3 Sources of Tungsten 8

2.4 Pricing 11

2.5 Applications [15] 12

2.6 Production of Tungsten 14

2.7 Electrochemical Production of Metals 18

2.8 Electrochemical Reduction of Tungsten Compounds 22

2.9 Pulse Current Applications 24

3.EXPERIMENTAL 27

3.1 Laboratory Scale Experiments 27

3.2 Large Scale Experiments 33

3.3 Post Electrolysis Work 37

4.RESULTS AND DISCUSSION 39
4.1 Laboratory Scale Experiments 39
4.2 Large Scale Experiments 57
5.CONCLUSIONS 65
5.1 Recommendations for the Future Work 66
REFERENCES 67

LIST OF TABLES

TABLES

Table 2.1 Some of the key properties of tungsten [8] 5
Table 2.2 Some of the most important minerals of tungsten [9] 8
Table 2.3 Some of the properties of scheelite [8] 9
Table 2.4 Some of the properties of wolframite group of minerals [9]. 10
Table 3.1 Experimental Parameters 32
Table 3.2 EDS analysis of the $CaWO_4$ (Noah, 18418) powder. 37
Table 4.1 Corresponding average potential values for 48wt% theoretical reduction of $CaWO_4$ 45
Table 4.2 Relative intensity values for the crystallographic planes of the samples from this study and commercial tungsten powder 52
Table 4.3 Relative intensities as percentages between four detected peaks 52
Table 4.4 Descriptive statistics of energy consumption values 54
Table 4.5 EDS analysis result of $CaWO_4$ powder after 0.1 M HCl cleaning 57

LIST OF FIGURES

FIGURES

Figure 1.1 a) Top metals and minerals of the supply risk index 2012, b) Risk index of a) in 2015. (0 very low - 10 very high risk of supply) Reproduced from [1]..... 1
Figure 2.1 Schematic flow of tungsten powder metallurgy. 6
Figure 2.2 Distribution of worlds tungsten reserves, 3 m tonnes W content [13] 11
Figure 2.3 Historical tungsten prices for the last two decades. Reproduced from [14] 12
Figure 2.4 Main uses of tungsten, global [15]..... 13
Figure 2.5 The flowsheet of the modern APT production steps from the concentrates and scrap..... 15
Figure 2.6 Flowsheet summary of tungsten metallic powder production from APT. 16
Figure 2.7 A schematic representation of the system for cathodic refining process.. 20
Figure 2.8 Schematic representation of cell design of FFC Cambridge Process; a-) pellets are placed at the bottom of the crucible that act as cathode and b-) pellets are attached to a cathode current collector 21
Figure 2.9 Represenetative pulse current waveform 25
Figure 3.1 The schematic representation of the cell..... 27
Figure 3.2 A photograph of the overall experimental setup..... 29
Figure 3.3 Phase diagram of the $CaCl_2$-NaCl system. Reproduced from [44]..... 30
Figure 3.4 Phase diagram of $CaCl_2$-H_2O system. Reproduced from [45]..... 31
Figure 3.5 A photograph of the system and alumina coated graphite..... 34
Figure 3.6 A photograph of the complete system 35
Figure 4.1 Voltage vs. time graphs for 0.3 A average current 40
Figure 4.2 Voltage as a function of charge (A.min) for the selected experiments..... 41
Figure 4.3 Potential values as a function of time for the first ten minutes of the experiments with 0.2 A average current..... 43

Figure 4.4 Potential values as a function of time for the first ten minutes of the experiments with 0.1 A average current 43
Figure 4.5 Voltage as a function of time for the experiments performed with 0.1, 0.2 and 0.3 A average current and fixed pulse relaxation time at 9 ms..... 44
Figure 4.6 XRD result of the cathode sample, I_{avg}=0.2 A, t_{off}=9ms 46
Figure 4.7 XRD result of the sample obtained from electrolyte, I_{avg}=0.2 A, t_{off}= 19 ms 47
Figure 4.8 X-ray diffraction pattern of a sample cleaned with 0.2 M HCl solution, I_{avg}=0.3 A, t_{off}=9 ms 48
Figure 4.9 SEM photograph of the raw material pellet ($CaWO_4$)..... 49
Figure 4.10 SEM photograph of the reduced powder I_{avg}=0.3 A, t_{off}=19 ms 49
Figure 4.11 SEM photographs of the samples produced with a-) I_{avg}=0.3 A, t_{off}=19ms b-) I_{avg}=0.2 A, t_{off}=9 ms c-) I_{avg}=0.3 A, t_{off}=1ms d-) I_{avg}=0.2 A, t_{off}=1ms..... 50
Figure 4.12 EDS analysis of the lath shaped particles obtained from I_{avg}=0.2 A, t_{off}=1ms..... 51
Figure 4.13 Estimated marginal means of energy consumption binary interaction plot 55
Figure 4.14 Profile plots for a) average current (I_{avg}) and b) pulse relaxation time (t_{off})..... 56
Figure 4.15 X-ray diffraction pattern of the produced and cleaned powder..... 58
Figure 4.16 Chronoamperogram of the experiment conducted with 60 grams of $CaWO_4$ 59
Figure 4.17 A photograph of the graphite electrode after electrolysis experiments .. 60
Figure 4.18 A photograph of the “boron nitride applied” graphite after the electrolysis..... 61
Figure 4.19 A photograph of the alumina coated graphite after the electrolysis experiments 62
Figure 4.20 X-ray diffraction pattern of the one of the produced samples..... 63
Figure 4.21 X-ray diffraction pattern of the one of the produced samples..... 63
Figure 4.22 SEM photograph of the produced tungsten 64

CHAPTER 1

INTRODUCTION

Material science and engineering is at the heart of raising technology. One of the most important considerations of a metallurgical and materials engineer is to focus on the engineering applications of materials. As a consequence of that, cost is a critical phenomenon that is determined by many factors for a materials usage in the engineering applications. Abundance in the nature which is one of the factors that directly affects it. Furthermore, a metallurgical and materials engineer should strongly consider the process development of low abundant materials to service them for engineering use.

Tungsten is one of the metals whose abundancy is decreasing, while importance is increasing due to the need for the engineering applications. It is among the elements that have very high risk of supply (See Figure 1.1.) which is determined by British Geological Survey by taking several factors such as reserve distribution, substitutability, recycling rate and etc. into consideration [1].

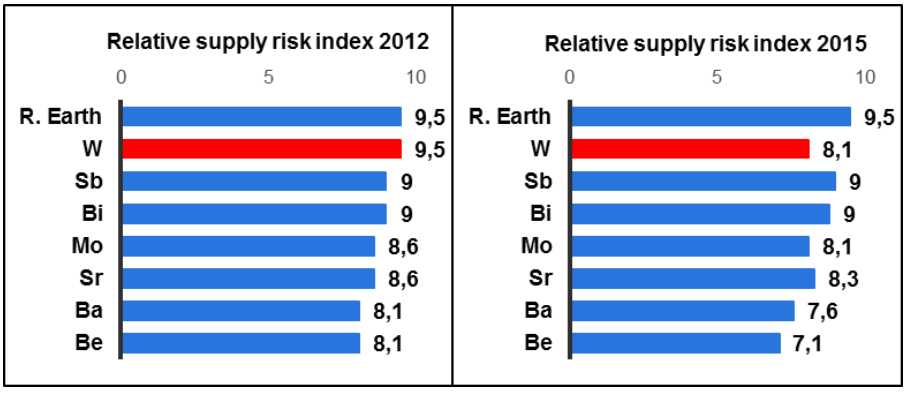


Figure 1.1 a) Top metals and minerals of the supply risk index 2012, b) Risk index of a) in 2015. (0 very low - 10 very high risk of supply) Reproduced from [1].

Currently, tungsten metal powders are produced via hydrogen reduction method in the industry. This reduction process demands tungsten oxides which are mostly provided by conversion of an intermediate product that produced from tungsten minerals which is ammoniumparatungstate (APT). Hydrogen reduction method is the only technically important method for tungsten production, but it has many difficulties that will be discussed later in Section 2.6.

Electrometallurgical methods in the metal production are preferred where the pyro-metallurgical and hydrometallurgical routes are not feasible. Furthermore, molten salt electrolysis is critical in production of some metals where electrowinning from the aqueous solutions is not possible to apply.

Molten salt electrolysis has been used in the metal production industry for over a hundred years. However, its importance has been on an increasing trend for last two decades since the development of FFC Cambridge process in 1997. The FFC Cambridge process is an electrochemical metal production method in which metal oxides or nitrides are directly reduced in molten salt electrolytes [2]. This process has the potential to develop a production route for certain metals and alloys including tungsten and its alloys, in a more efficient way than the currently applied conventional production processes [2]. As a result of this, several studies were performed to develop an alternative route for tungsten production that is to be discussed in Section 2.8.

Erdoğan and Karakaya reported the electrochemical reduction of $CaWO_4$ (scheelite) to metallic tungsten for the first time [3–7] . Considering the abundance of raw materials and the ease of the process, this novel process is possessing high potential as an alternative promising tungsten powder production route as proven by several studies (discussed in Section 2.8).

1.1 Aim of this study

The aim of the laboratory scale part was to perform studies to improve the electrode kinetics in the tungsten production technique mentioned above [3]. By the application of pulse current, it was targeted to achieve higher reduction yield and energy efficiency. Since there is very limited literature on the pulse application for electrochemical processes in molten salts, the findings of this thesis will contribute directly to the literature.

The second part included studies to increase the production capacity above laboratory scale. It was aimed to collect information about the difficulties which could be encountered in pilot and/or industrial scale production. Contribution to the development of a new production technique for one of the most strategic metals, tungsten, was the main motivation. Furthermore, the collection of larger volume of tungsten powder produced by above mentioned method could open the way to test them for further studies.

CHAPTER 2

LITERATURE REVIEW

2.1 Tungsten

Tungsten has the highest melting point and the lowest coefficient of thermal expansion of all metals. Moreover, tungsten is remarkable for its very high density, moduli of compression and elasticity, moderate electrical and thermal conductivity, thermal creep resistance and good high temperature mechanical properties. Some of the key properties and other features are given in Table 2.1. [8].

Table 2.1 Some of the key properties of tungsten [8]

Atomic number	74
Atomic weight	183.84
Electron configuration	{Xe} $4f^{14}$ $5d^4$ $6s^2$
Atomic radius	137 pm
Lattice parameter	a=3.16524 Å (298 K)
Density	19.25 g/cm^3 (298 K)
Melting point	3422±15°C
Boiling point	5700±200°C
Crystal structure	Body-Centered Cubic A2
Electrical resistivity	5.28 μΩ•cm
Specific heat capacity	135 J•kg^{-1}•K^{-1} (298 K)
Enthalpy of fusion	46 kJ•mol^{-1}
Thermal conductivity	1.75 •W•cm^{-1} •K^{-1}(298 K)
Coefficient of thermal expansion	4.32-4.68×10^{-6}•K^{-1}(298K)
Hardness	300-650 HV30, 7.5 Moh
Modulus of elasticity	390-410 GPa (298 K)

Tungsten is a metal of powder metallurgy. As a consequence of having the highest melting point of all metals, melting and casting is not applied. Hence, tungsten mill products such as sheets, rods, pins and wires are fabricated by routes of powder metallurgy which is embraced from ceramics. Some of the steps of the powder metallurgy are given in Figure 2.1. As it can be seen in Figure 2.1, these routes contain steps like powder pressing, sintering and machining (forging, rolling, swaging, wire drawing, etc.)

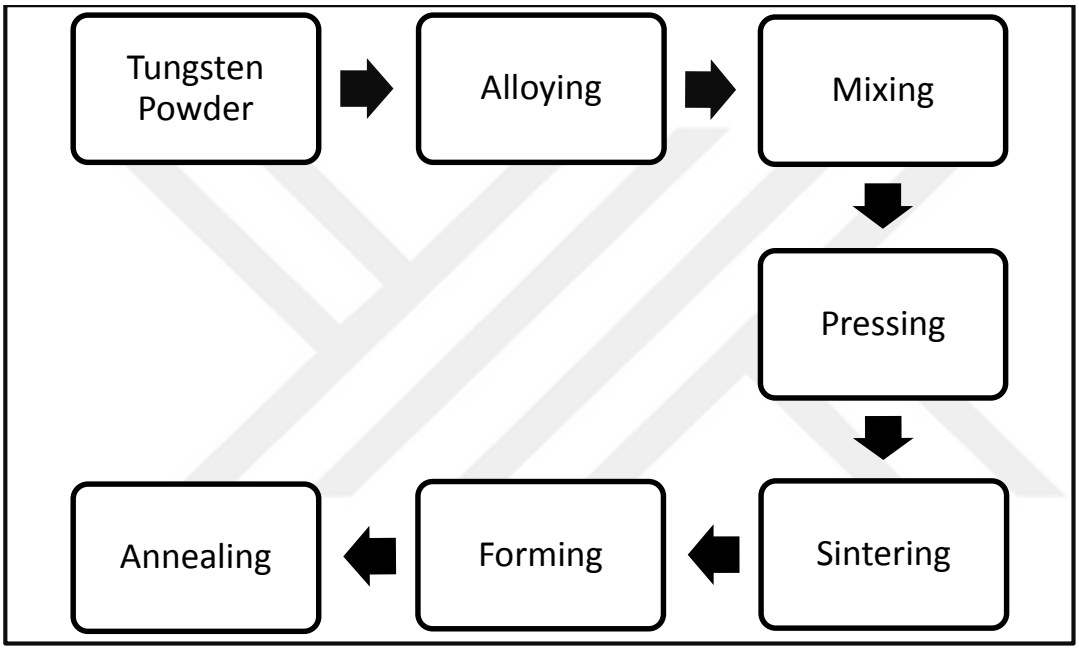


Figure 2.1 Schematic flow of tungsten powder metallurgy.

2.2 History of Tungsten [9]

Wolframite, which is a mineral of tungsten, was already known in the tin mines of Saxony and Bohemia before the discovery of elemental tungsten in 1783. First thought was a tin mineral that contained iron and arsenic by Ercker in 1574. The origin of the wolfram name was deduced from the word wolf. In 1575, a new high density mineral was portrayed as a calcium-containing iron mineral by Cronstedt and was called as “tungsten” which means heavy stone in Swedish (*tung sten*).

W. Scheele investigated the mineral and proposed digestion and precipitation with acid to decompose the mineral into metal in 1871 that Bergmann proposed carbon reduction later in the same year. Deelhuyar brothers produced the element from wolframite mineral and named it wolfram in 1783. Scheelite name was proposed for $CaWO_4$ mineral by Leonhard in 1824.Oxland obtained a patent in 1874. In this patent, production of sodium tungstate, tungsten oxide and metallic tungsten were included. In addition, mention of ferrotungsten production took place for the first time. The industrial use of tungsten was launched with the developments starting from the production of WC by Moissan in 1890. They may be chronologically summarized as follows:

Bethlehem Steel Company announced the first high-speed, high-temperature steel at the Paris Exhibition in 1900.

The first tungsten filaments for lamps were manufactured in Hungary according to patent by Just and Hanamann in 1903.

Production of ductile tungsten wires by powder metallurgy was portrayed by W. D. Coolidge in the patent of 1909. This process was the first time use of powder metallurgy for industrial applications that heritage of this process is still on charge in today industrial use.

The Osram Research Association obtained a patent for tungsten carbide – cobalt hard metals production of in 1922. After four years, the Krupp organization announced the first hard metal cutting tool.

The demand for tungsten increased due to the increasing use of hard metals in the steel machining, mining and armaments industry. As a result of this, raw materials supply and availability undergone in crisis situations and that provided the tungsten metal strategic importance. The tremendous military demands for heavy equipment, steel tools and weapons, armor plate, armor piercing shells was ranked the tungsten among world's strategic metals in the first half of the 20^{th} century and especially during the World War II [10] .

The trade of tungsten was restricted as a consequence of being strategic metal by Missile Technology Control Regime [11] and Wassenaar Arrangement [12].

2.3 Sources of Tungsten

The sources of tungsten have two main distinctions namely primary tungsten (ore concentrates) and secondary tungsten (types of tungsten containing scrap).

Tungsten is found in the earth's crust with a concentration of 1-1.5 ppm and considered as a rare metal. Tungsten's presence in the nature is only in the combined form. There are more than thirty minerals of tungsten in the nature. Some of the important minerals can be seen in the Table 2.2 [9].

Table 2.2 Some of the most important minerals of tungsten [9]

Name of the mineral	**Chemical formula**
Anthoinite	$Al(WO_4)\ (OH).\ H_2O$
Cuprotungstite	$Cu_2(WO_4)\ (OH)_2$
Ferritungstite	$Ca_2Fe_2^{+2}\ Fe_3^{+2}\ (WO_4)_7.\ 9H_2O$
Raspite	$PbWO_4$
Russellite	Bi_2WO_6
Sanmartinite	$ZnWO_4$
Scheelite	$CaWO_4$
Stolzite	$PbWO_4$
Tungstenite	WS_2
Tungstite	$WO_3\ .\ H_2O$
Ferberite	$FeWO_4$ with up to 20% $MnWO_4$
Hübnerite	$MnWO_4$ with up to 20% $FeWO_4$
Wolframite	$(Fe, Mn)WO_4$

As it can be seen from Table 2.2 [9], all the minerals are tungstates except tungstenite. Among them, only scheelite and the wolframite group of minerals are industrially important.

Scheelite reflects UV light as blue fluorescent that is very beneficial for ore detection and mining [9]. Some of the properties of scheelite are given in Table 2.3.

Table 2.3 Some of the properties of scheelite [8]

Formula		$CaWO_4$
WO_3 Content		80.6 %
Crystal Structure		tetragonal dipryramidal
Lattice Parameters	**a**	5.24-5.26 Å
	c	11.37-11.40 Å
	c/a	2.163-2.169 Å
Specific Gravity		5.9-6.1
Color		colorless, yellow, white, tan, orange, blue, black
Tenacity		very brittle
Luster		vitreous or resinous
Fracture		uneven
Hardness		4-5 Mohs
Magnetism		nonmagnetic
Streak		white
Diaphaneity		transparent or translucent

Iron and manganese containing tungstates are called as wolframite group of minerals. As it can be seen from Table 2.2, composition is a parameter for name determination of wolframite group of minerals such as ferberite and hübnerite [9]. Some of the properties of wolframite group of minerals are given in Table 2.4. Tungsten sources are spread across many different geographical locations in earth's crust. Major deposits are in the fold belts starting from the Far East to South China where the largest scheelite mine in the world is situated. Other important deposits are in Canada, USA, Bolivia, and Peru from Circumpacific belt. In addition, alpine fold

belt from France to Turkey and eastern costal fold belt in Australia are where the tungsten presented significant amounts [8]. Distribution of the world's tungsten reserves is indicated in Figure 2.2.

Table 2.4 Some of the properties of wolframite group of minerals [9].

		Ferberite	**Wolframite**	**Hübnerite**
Formula		$Fe(WO)_4$	$(Fe,Mn)WO_4$	$MnWO_4$
WO_3 Content		76.3 %	76.5%	76.6%
Crystal Structure		monoclinic	monoclinic	monoclinic
Lattice Parameters	**a**	0.471 nm	0.479 nm	0.485 nm a
	b	0.570 nm	0.574 nm	0.577 nm c
	c	0.574 nm	0.499 nm	0.498 nm a/c
	β	90º	90º26'	90º53'
Density		7.5 g/cm^3	7.1–7.5 g/cm^3	7.2-7.3 g/cm^3
Color		black	dark grey-black	red-brown black
Hardness		5 Mohs	5- 5.5 Mohs	5 Mohs
Common Form		well-formed crystals or masses	irregular crystal masses or radiating crystal groups	radiating groups of lamellar crystals

Secondary sources of tungsten

Recycling from scrap is one of the fundamental impact factors in world's tungsten supply. Estimated recycling rate is approximately 35% and since the scrap contains high amount of tungsten when compared to minerals, tungsten containing waste and scrap is a quite valuable raw material [8].

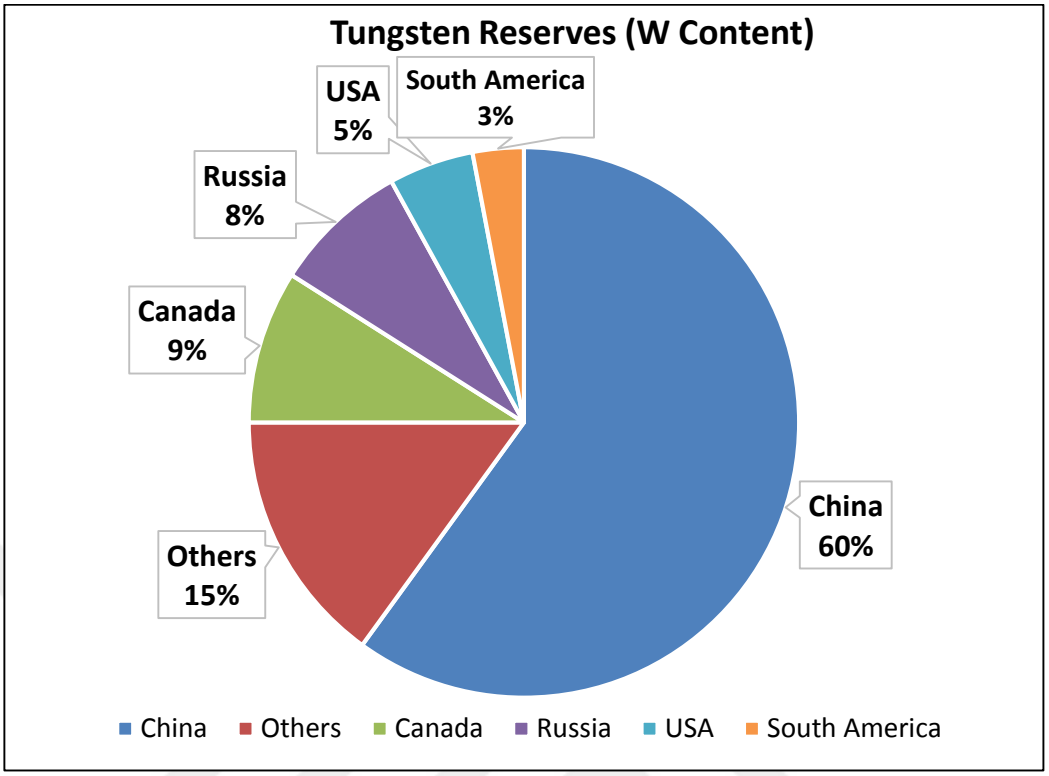


Figure 2.2 Distribution of worlds tungsten reserves, 3 million tonnes W content [13]

2.4 Pricing

Historical pricing data of tungsten in the last two decades is given in Figure 2.3. As it can be seen in this figure, there was a big increase in the prices in 2005. Another increase in prices is seen in 2011 from 245 to 460 US$/MTU. However, it came back to around 250 US$/MTU and still staying at this level. Prices are generally quoted per metric ton unit ("MTU" - one hundredth of a metric ton of 1,000 kilograms) of contained tungsten trioxide (WO_3). One MTU contains 10 kilograms of tungsten trioxide (WO_3) and/or 7.93 kilograms of tungsten (W).

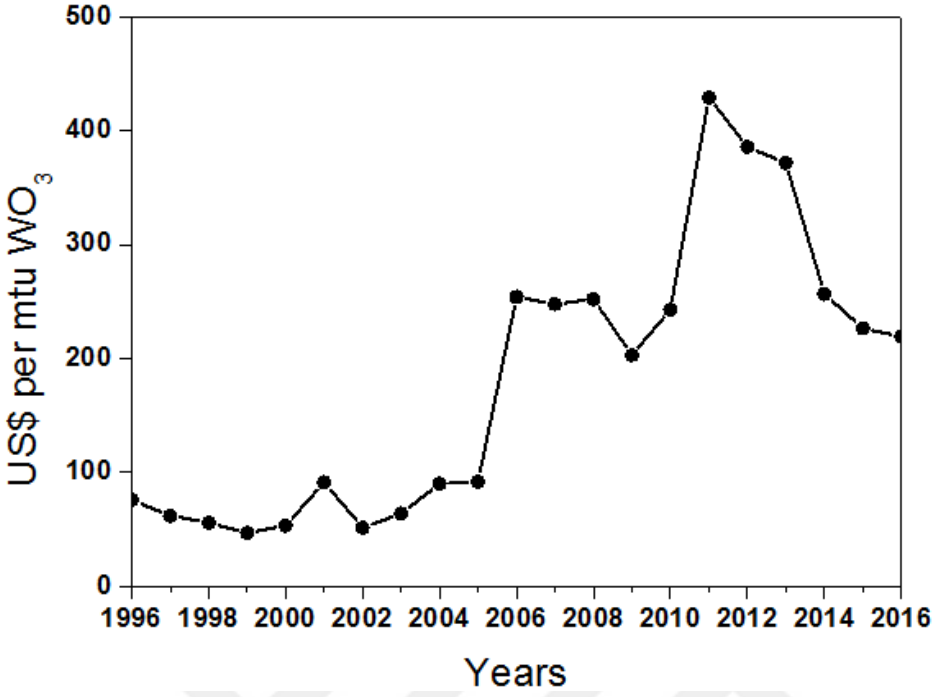


Figure 2.3 Historical tungsten prices for the last two decades. Reproduced from [14]

2.5 Applications [15]

Due to its unrivaled properties such as its melting point, density, coefficient of expansion and etc., tungsten acts as a critical element in a wide range of components for diverse applications. The main uses of tungsten are given in Figure 2.4. The main branches of tungsten applications are as follows;

Hard metals which consist tungsten carbide and cemented carbides. They have very high hardness, toughness and abrasion resistance. Therefore, they are used for drilling, cutting and coating applications such as punches, drill tips, millers and glass cutters.

Steel which is one of the most important engineering materials contains tungsten as an alloying element in its special forms such as high speed steels, tool steels and heat resistant steels to enhance its properties. They are mainly used for metal cutting and

special engineering applications that hardness and strength are needed especially around high temperature range.

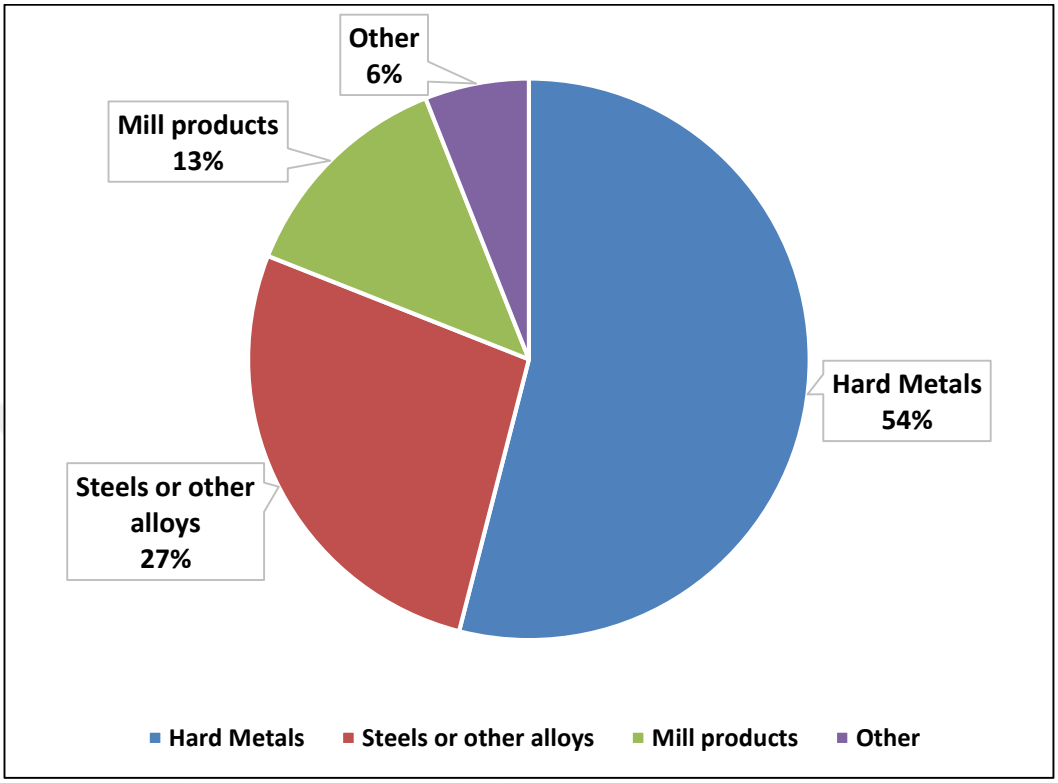


Figure 2.4 Main uses of tungsten, global [15]

Superalloys are performance enhanced solid solutions with special applications in the aerospace, marine turbine and industrial gas turbine industries where very high corrosion and wear resistance are extremely needed.

Tungsten heavy alloys (WHA) are generally tungsten-nickel-iron containing alloys that have a wide range of use where various properties such as very high density, strength, ductility, corrosion resistance, radiation adsorption capacity and high toughness are needed. Common examples of the WHAs include tungsten-copper (WCu) alloys for electrical contacts, high voltage switches; nickel-tungsten (WNi) alloys for coating shock absorbers, print rolls, portable electronic convertors. In addition, several important WHAs exist such as, tungsten-rhenium (WRe), tantalum-tungsten (TaW), molybdenum-tungsten (MoW) and niobium-tungsten (NbW) for X-

ray radiation shields, counter weights, vibration damping devices, heavy duty electrical contact materials and etc.

Mill products refer to sheets, rods or wires of tungsten. Due to having both extremely high melting point, good conductivity and ductility at the same time, pure metallic tungsten is quite reasonable choice for electrical and electronic applications such as incandescent light bulb filaments, heating elements and vacuum tubes. Moreover; electrical contacts, circuit interconnects, furnace filaments and welding applications are other examples of mill products.

Chemicals and other specialist applications are also a division where tungsten is presented. Reaction catalysts and pigments are the common examples of this division.

2.6 Production of Tungsten

Production of metallic tungsten powder is divided into two main categories: Production from concentrates (primary tungsten sources) and production from scrap (secondary tungsten sources).

2.6.1 Production from Concentrates

Scheelite and wolframite concentrates undergo dissolution steps via alkaline pressure digestion by using concentrated NaOH solution or soda to obtain sodium tungstate solution. The solution is then purified by filtration and precipitation prior to conversion into ammonium tungstate by solvent extraction or ion exchange resins. Eventually, high purity ammoniumparatungstate (APT) is obtained subsequent to crystallization steps [8]. The flowsheet of the APT production steps from the minerals can be seen on Figure 2.5.

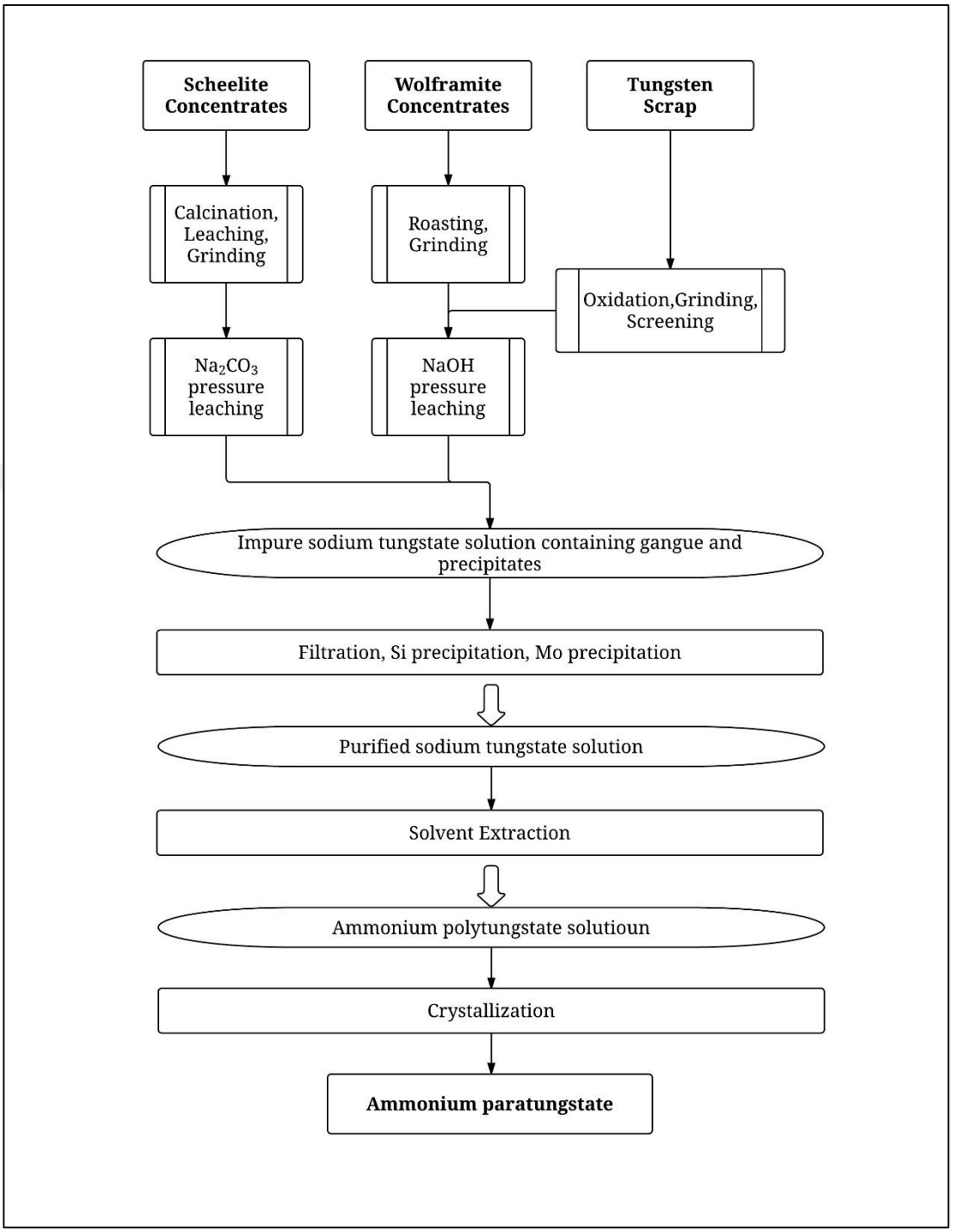


Figure 2.5 The flowsheet of the modern APT production steps from the concentrates and scrap.

APT (chemical formula: $(NH_4)_{10}(H_2W_{12}O_{42})4H_2O$) is a vital intermediate product for the industrial tungsten production. APT is converted into tungsten oxides via calcination generally in rotary furnaces. The flowsheet of the conversion process is given in Figure 2.6

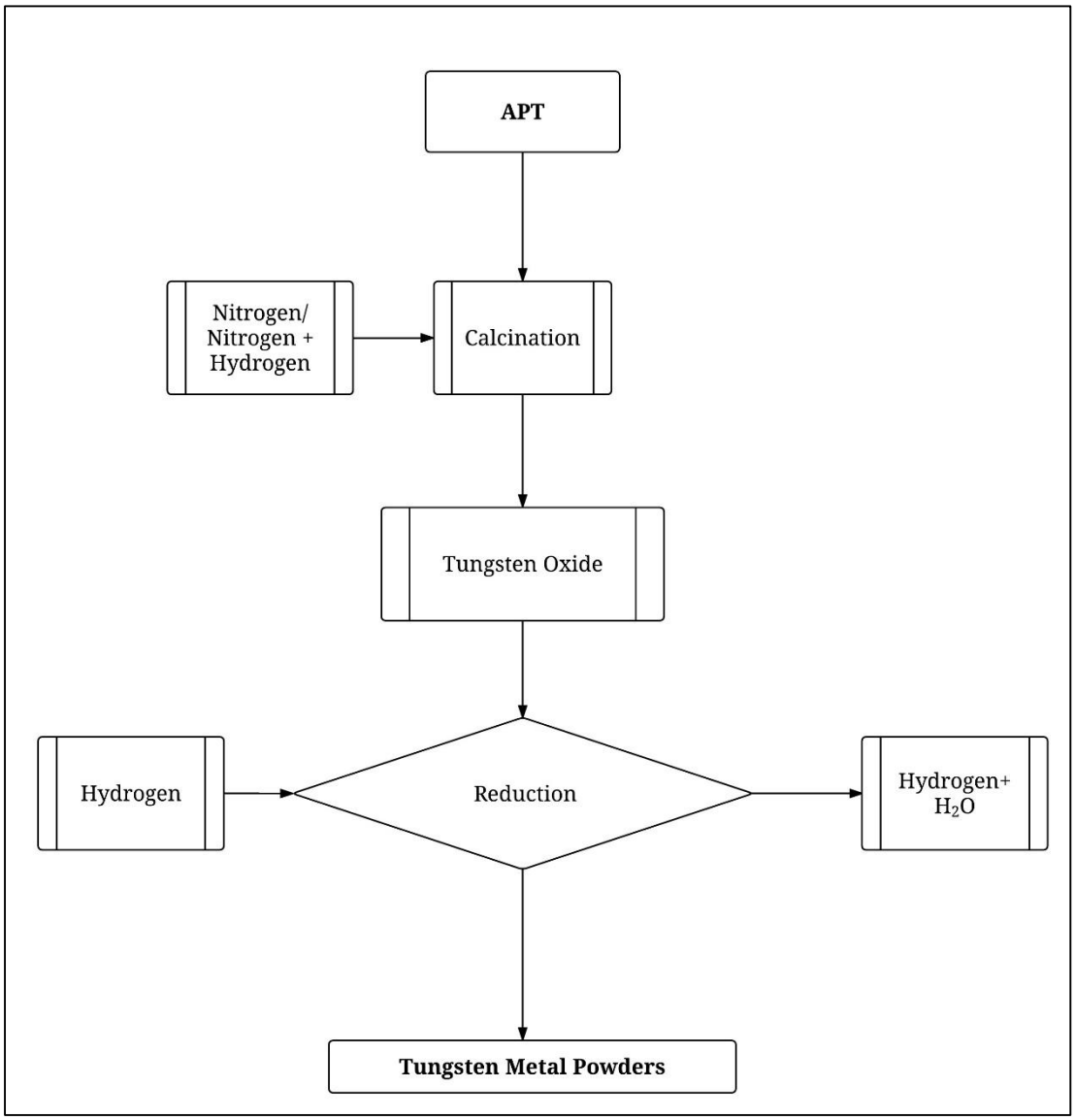


Figure 2.6 Flowsheet summary of tungsten metallic powder production from APT

The WO_3 obtained by the conversion process is reduced to metallic tungsten powder in controlled hydrogen atmosphere in the temperature range of 600 to 1100°C. The hydrogen reduction of tungsten includes the following steps;

$$WO_3(s) + 0.1H_2 \longrightarrow WO_{2.9}(s) + 0.1H_2O \quad (2.1)$$

$$WO_{2.9}(s) + 0.18H_2 \longrightarrow WO_{2.72}(s) + 0.18H_2O \quad (2.2)$$

$$WO_{2.72}(s) + 0.72H_2 \longrightarrow WO_2(s) + 0.72H_2O \quad (2.3)$$

$$WO_2(s) + 2H_2 \longrightarrow W(s) + 2H_2O \quad (2.4)$$

$$WO_3(s) + 3H_2 \longrightarrow W(s) + 3H_2O \quad (2.5)$$

Currently, hydrogen reduction is the only method for the metallic tungsten production in the industry. The reduction takes place in the industrial pusher furnaces or rotary furnaces which have a temperature control zones between 600 and 1100 °C. Hydrogen is constantly supplied to act as a reducing agent and to carry away the water vapor formed by the reactions. The final product grain size is controlled by temperature, H_2 flow rate, heating time and oxide quantity. Commercial tungsten powders are in the size range of 0.1 to 100 μm. The purity of the powders is directly related to the purity of APT that was formed before the reduction processes.

Hydrogen is superior to other reducing agents for the end product purity that directly affects the further processing of tungsten products. Since the purity is related with the reducing agent, metallothermic and carbonothermic reduction of tungsten oxides are not preferred in metallic tungsten powder production. However, hydrogen reduction has several drawbacks. As it can be seen from Figure 2.5 and Figure 2.6 the overall process has many steps that consume lots of time and energy. Besides, the driving force of the reduction reaction is relatively low, because the Gibbs Free Energy difference is not a large negative value. In addition, the reduction reactions are endothermic and require continuous heat supply. Furthermore, hydrogen is a dangerous gas to handle that requires serious health and safety considerations.

2.6.2 Production from Scrap

Due to high tungsten contents, scrap is valuable raw material when compared to minerals. However, direct tungsten recycling from scrap is not possible. That's why tungsten scraps are oxidized and converted into APT for further processing in the routes of hydrogen reduction. The steps involved in the conversion of scrap into APT are also illustrated in Figure 2.5.

2.7 Electrochemical Production of Metals

Molten salt electrolysis is used in the metal production industry especially where the pyro-metallurgical and hydrometallurgical routes are not feasible to apply. In molten salt electrolysis, the starting compound that contains the metal for electrowinning is first dissolved in the electrolyte. Next, electrowinning of the metal from solution is provided by the application of direct current.

The process is more suitable for low melting point metals because they can be obtained in liquid state. On the contrary, electrowinning of high melting point metals will be in solid state because the reduction temperature is lower than the melting point. As a result, dendritic deposition is inevitable in most of the cases. Although molten salt electrolysis of many oxides, chlorides and fluorides are possible the applications of the process in industrial scale is quite limited especially due to the corrosive nature of the molten salts. Magnesium production from its chloride salts is the most important example of molten salt electrolysis of chlorides. Moreover, aluminum production from its oxides is the only industrially important example of the molten salt electrolysis of oxides.

There is a patent taken for tungsten production by molten salt electrolysis in 1966 [16]. The claim involved dissolving the starting material ($CaWO_4$) into the electrolyte and deposition of tungsten at the cathode. However, this process was not practically useful for the metallic tungsten production in the industry due to dendritic

structure of deposited tungsten. Furthermore, the tungsten product was not suitable for further processing like pressing and sintering.

As a whole, molten salt electrolysis has some disadvantages such as dendritic deposition, oxygen contamination of products when exposed to air and increased activity of redox reactions. The most serious outcome of tungsten electrowinning was arisen from the coarse particle size of the electrowon tungsten [17].

2.7.1 Oxygen Removal from Metal Oxygen Solid Solutions

Ward and Hoar [18] reported a novel cathodic refining technique in 1960. By this technique, oxygen and other impurities could be eliminated from the cathode in a $BaCl_2$ electrolyte with the application of a potential that is higher than the decomposition potential of $BaCl_2$ electrolyte. A schematic representation of the system for cathodic refining process is given in Figure 2.7

Overall cell reaction for copper refining was proposed as;

$$Cu_2X + BaCl_2 \longrightarrow 2\,Cu + BaX + Cl_2 \qquad (2.6)$$

Where X is the undesired element such as oxygen.

Okabe et al [19–21] investigated the removal of oxygen from oxide compounds of titanium in molten calcium chloride by pursuing similar conditions to study of Ward and Hoar [18]. The studies indicated that the reductant calcium metal was formed as a consequence of the electrolysis of calcium chloride providing up to 10 ppm of oxygen impurity level.

Calcium metal which is the product of the electrolysis is reacted with oxygen and end up as calcium oxide (CaO). This oxide is dissolved in the salt for further Ca electrolysis.

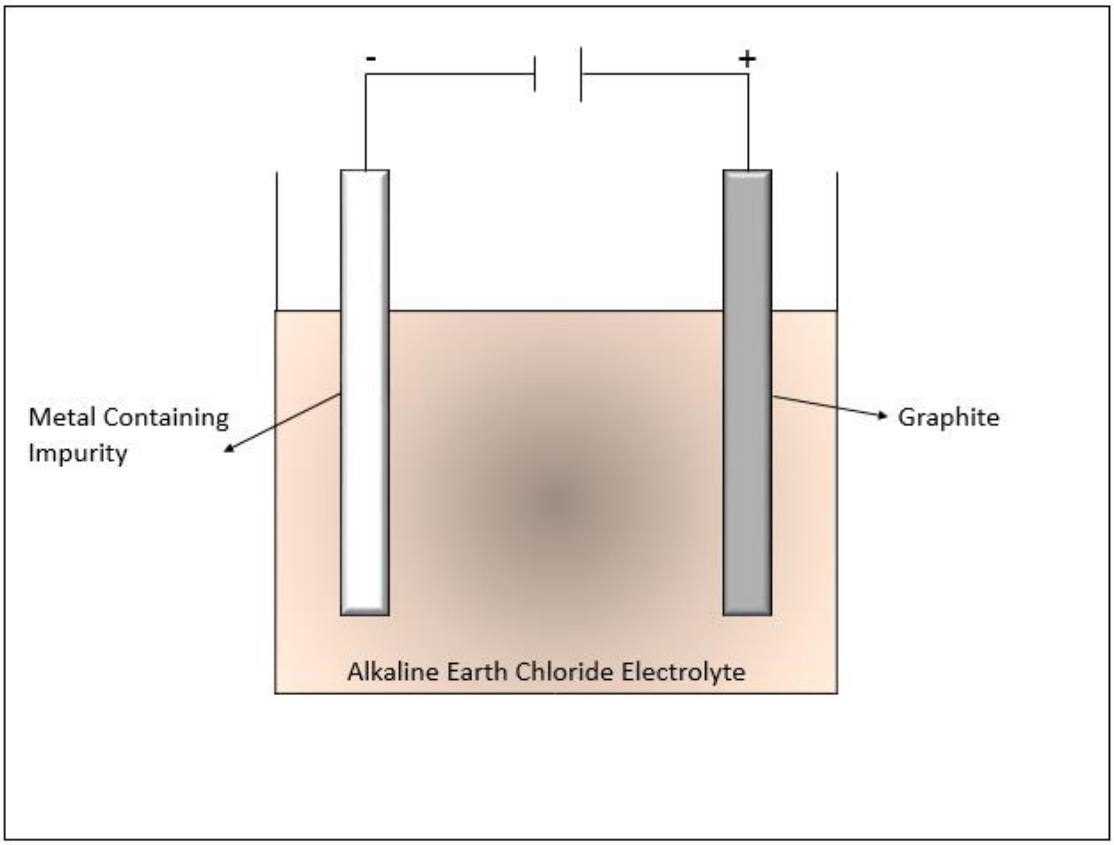


Figure 2.7 A schematic representation of the system for cathodic refining process

2.7.2 FFC Cambridge Process

An innovative process for the electrochemical production of metals in molten salts from their compounds like oxides, sulphides, carbides or nitrides was reported in 1997 [2]. This high temperature electrolysis process in molten salt is named as FFC (Fray-Farthing-Chen) Cambridge process. The representative image for the cell design of FFC Cambridge process is given in Figure 2.8. Graphite is used as the anode and a metal compound is used as the cathode in a molten salt medium that contains calcium chloride.

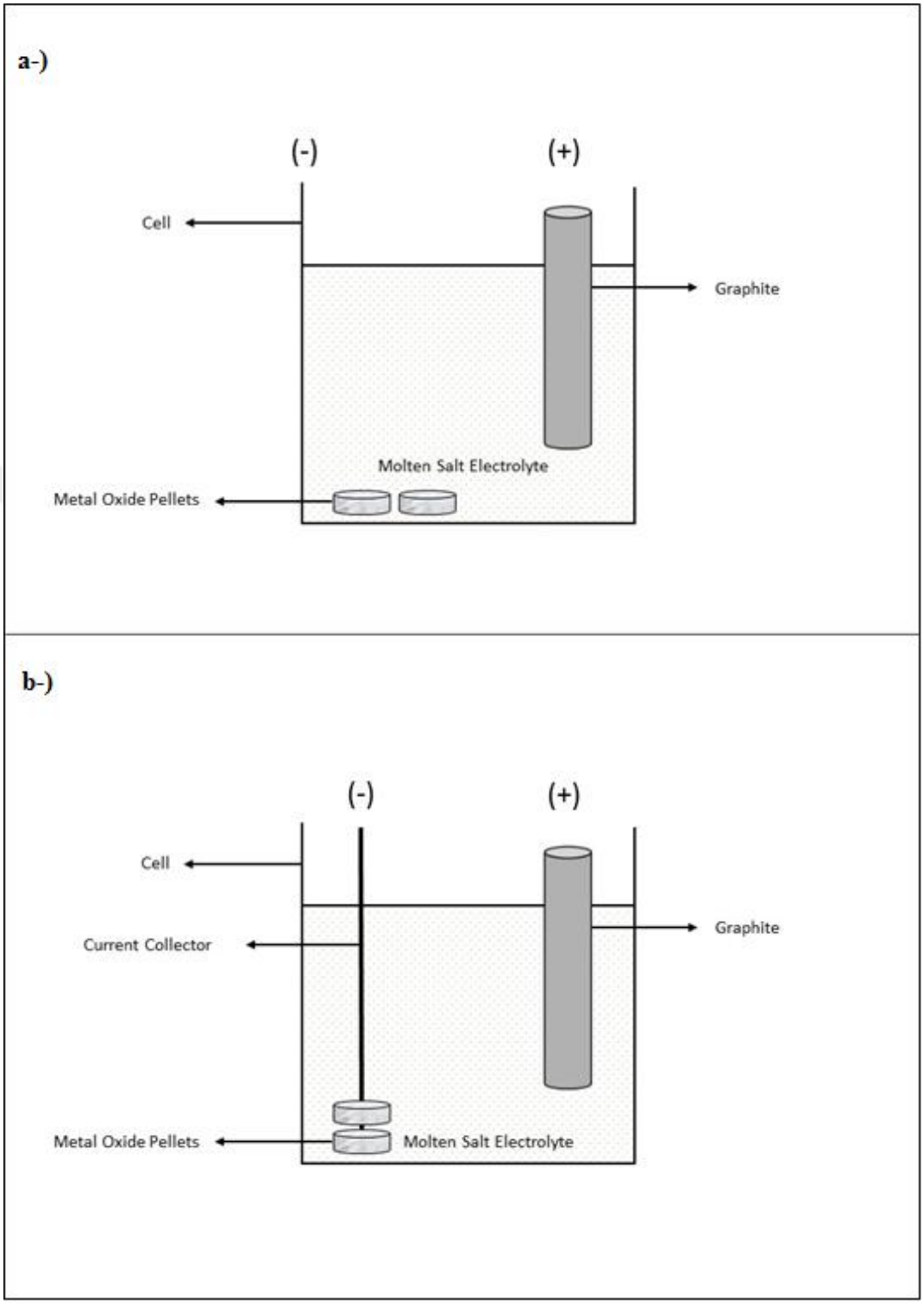


Figure 2.8 Schematic representation of cell design of FFC Cambridge Process; a-) pellets are placed at the bottom of the crucible that act as cathode and b-) pellets are attached to a cathode current collector

Applied potential difference is lower than the decomposition potential of the molten salts. However, it is higher than the decomposition potential of the metal compound at the cathode. By this way, undesired ions are removed from the cathode and formed a compound with the carbon which is introduced by graphite anode.

It is stated that this process is more suitable for electrochemical production of high melting point metal oxides and actinides [22]. Yet, metal oxides are the only accountable compounds for metal production studies most of the time. The general forms of the reactions are as follows;

$$yO^{-2} + yC\,(s) \longrightarrow yCO(g) + 2ye^{-} \quad \underline{OR} \qquad (2.7)$$

(anode)

$$yO^{-2} + y/2C\,(s) \longrightarrow y/2CO_2(g) + 2ye^{-} \qquad (2.8)$$

$$A_xO_y(s) + 2ye^{-} \longrightarrow xA\,(s) + yO^{2-}\,(g) \qquad \text{(cathode)} \qquad (2.9)$$

$$A_xO_y(s) + yC(s) \longrightarrow xA\,(s) + yCO\,(g) \quad \underline{OR} \qquad (2.10)$$

(overall)

$$A_xO_y(s) + y/2C(s) \longrightarrow xA\,(s) + y/2CO_2\,(g) \qquad (2.11)$$

Fray-Farthing-Chen (FFC) Cambridge process has been reported as successful for the laboratory scale electrochemical production of Titanium [22], Chromium [23], Silicon [24], Copper [25], Aluminum, Boron, Iron, Vanadium, Niobium, Uranium, Neodymium, Zirconium, Hafnium, Cerium, and Nickel [27–29] from their compounds.

2.8 Electrochemical Reduction of Tungsten Compounds

There have been some studies reported for the electrochemical reduction of tungsten compounds to produce tungsten alloy by molten salt electrolysis.

Dring et al. reported the production of Ti-10 wt% W alloy via electro-deoxidation of mixed TiO_2+WO_3 which is used as a raw material in a molten $CaCl_2$ electrolyte at 900^oC [29].

Bhagat et al [30] reported the loss of WO_3 and proposed the reactions as follows,

$$WO_2 = WO^{2+} + O^{2-} \quad (2.12)$$

$$WO_3 = (WO_2)^{2+} + O^{2-} \quad (2.13)$$

They emphasized that the losses were to the electrolyte because of the formation of oxychloride and chloride phases. On the contrary, Erdoğan and Karakaya [3] reported the formation of WO_2Cl_2 while conducting similar experimental procedure for the reduction of WO_3. The proposed reaction was as follows;

$$2\ WO_3\ (s) + CaCl_2\ (l) = CaWO_4\ (s) + WO_2Cl_2\ (g) \quad (2.14)$$

They reported the oxychloride phase was in gaseous state and deposited in the cold parts of the cell vessel as yellow powders. They also reported that the loss of starting material was almost 50 wt % according to proposed reaction. As a result, production of tungsten metallic powders by the reduction of WO_3 is not possible without the material loss due to reaction between calcium chloride and tungsten trioxide that yields volatile oxychloride of tungsten. In addition, conversion of WO_3 into $CaWO_4$ is expected due to proposed reaction. Since the dissolution of starting material into the electrolyte was not desired for the direct electrochemical reduction of metal oxides, the incomplete reduction was explained with the 15 % mole solubility of $CaWO_4$ in molten $CaCl_2$ at 900 ^oC [31].

Erdogan and Karakaya reported that formation of metallic tungsten powders was due to the reduction of $CaWO_4$. That's why, the reduction of $CaWO_4$ was investigated by putting CaO and WO_3 into a reaction to form $CaWO_4$ as a starting material. The proposed electrolyte was consisting of $CaCl_2$-NaCl salts at the eutectic composition considering the low solubility of $CaWO_4$ at around the temperature of 600^oC. It was

reported that there was no significant solubility (1% mole) of CaWO4 either in molten NaCl or $CaCl_2$ at around the reaction temperature [32]. It was indicated for the first time that production of tungsten metallic powder was feasible via direct electrochemical reduction of $CaWO_4$. The product was washed with HCl to eliminate the byproducts of the electrolysis.

With this novel tungsten production technique, several studies were reported. Tang et all [33] reported the production of fine tungsten powder having particle size less than 200 nm under the same conditions. They reported the dissolution of any residual unreduced $CaWO_4$ during washing stage which was performed after the electrolysis. As a consequence, they reported that, the metallic tungsten powder was obtained with high yield (95-97.42%) [33].

In 2014, Tran-Nguyen et al [34] reported the production of tungsten carbide using experimental conditions very similar to the one used by Erdoğan and Karakaya [3]. Tungsten carbide is produced by the carburization of tungsten. They used $CaWO_4$/C precursors as raw material. The production of tungsten carbide reported by in situ chemical reaction of carbon and electrochemically produced tungsten via reduction of $CaWO_4$ at 1173 K.

2.9 Pulse Current Applications

The electrochemical reduction of the solid oxides by FFC process involves oxygen ionization and hence the deoxidation at the solid oxide-molten electrolyte-metal interface. Therefore, the oxygen ions from the metal oxide should diffuse to the interface. The rate-limiting step was reported as the diffusion of oxygen in the solidoxide by previous studies [2, 22, 29, 36].

There is very limited literature detected by the author for the pulse current application either in tungsten production or metal production from their compounds. Generally, pulse concept is mainly used in electrodeposition applications. The potential or current is rapidly alternated between two selected values. By doing so, a

set of pulses that distinguished by zero current is generated with the same amplitude and duration [37, 38]. Each pulse originated from an on-time (t_{on}) which current is applied in this duration, and an off-time (t_{off}) which zero current is applied in this duration as shown in Figure 2.9.

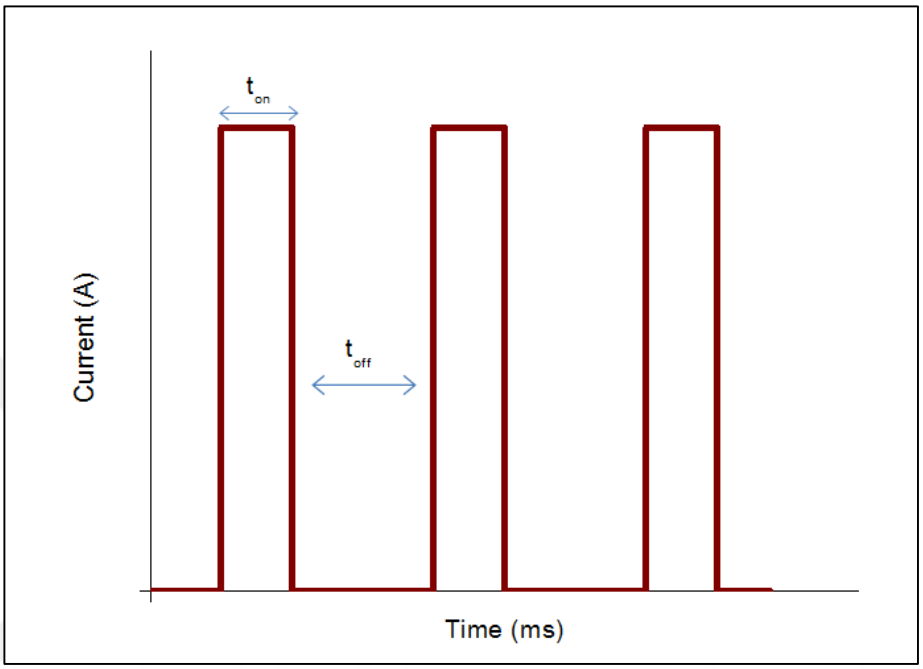


Figure 2.9 Represenetative pulse current waveform

The deposited film composition and thickness are reported as controllable in atomic order via regulating the pulse amplitude and width 39–41]. The initiation of grain nuclei is favored and the number of grains per unit area resulting in finer grained deposit is increased resulting improved properties as compared to direct current coating applications [37].

High peak current increases the population of atoms and nucleation rate in pulse electrodeposition. Pulse current can influence the mechanism of crystallization and varies the physical and mechanical properties of the electrodeposited substance.

The nuclei formation rate is determined by [41];

$$\upsilon = K_1 \exp\left(-K_2/\eta\right) \tag{2.15}$$

where K_1 is proportionality constant, K_2 including peak current is the activation energy required for nucleation and η is the overpotential of crystallization.

Referencing the above equation, it can be stated that peak current is directly proportional to the overpotential. As a result, increasing the peak current has a positive effect on obtaining finer crystals. Current interruptions via pulse off time enables the re-nucleation because of the removal of impurities [37].

Pulse current can also affect the composition of the alloy deposited. The deposit alloy may indicate a composition modulation during on and off time [42]. By this way, composition modulated and ternary alloys can be produced by pulse current.

There are significant advantages of pulse current in the electrochemical applications. It is reported that, modification of pulse parameters was provided to obtain deposits having desired composition, porosity, structure and hydrogen content in pulse electrodeposition studies [38, 44]. Pulse plating decreases the need to use additives by 50–60%.

There are also minimal reported disadvantages of pulse current and pulse reverse techniques. The cost of the pulse rectifier is usually greater than a direct current unit. The considerations in the sophisticated and regulated design with significant tolerances costs more to manufacture. The planning and organization of the procedures should be seriously considered to obtain best results [37].

CHAPTER 3

EXPERIMENTAL

The experimental studies were divided into two parts as laboratory scale experiments and the larger scale experiments. Laboratory scale experiments could be considered as the simulation of the larger scale experiments due to the ease of application when compared to larger scale experiments. The detailed experimental designs and parameters are illustrated in this chapter.

3.1 Laboratory Scale Experiments

The schematic representation of the cell is shown in Figure 3.1.

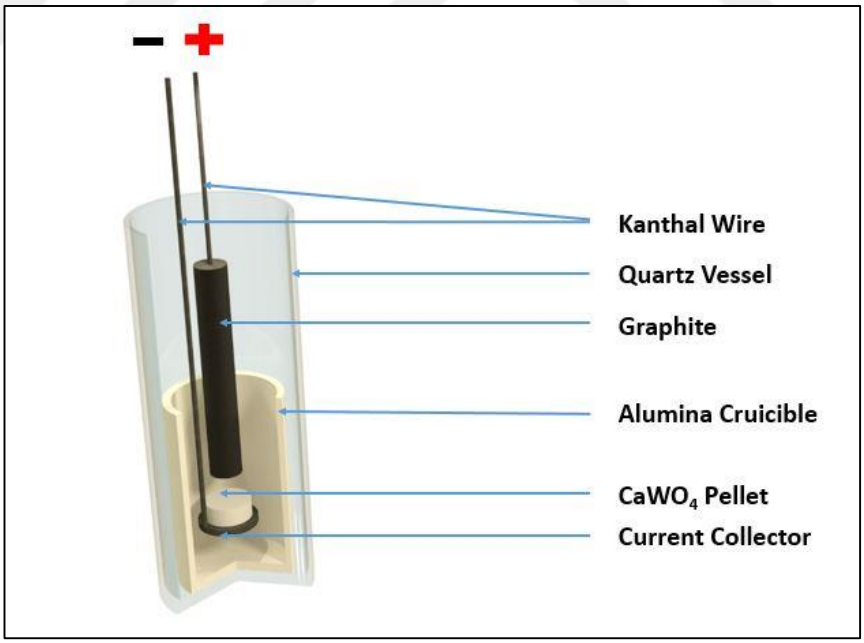


Figure 3.1 The schematic representation of the cell

2.5 grams of commercially available $CaWO_4$ powder (Aldrich 24.866) was dry pressed under 2 tons of load to form a pellet of with 1.5 cm diameter and 0.3 cm height. The $CaWO_4$ pellet was placed into a spoon (stainless steel) having 2 cm diameter and 0.6 cm height. Spoon was welded to the end of a 3 mm diameter stainless steel wire for the cathode assembly. This wire was covered with an alumina insulator near to the contact zone to prevent any short circuit problem during the experiment. A 13 mm diameter and about 18 cm long graphite rod (Alfa Aesar A10134) was used as anode material. An alumina crucible of an outside diameter of 4 cm and height of 10 cm was placed to contain the molten salt medium. Alumina was selected due to being resistant to reaction temperature and corrosive molten medium.

The cell was positioned in a high temperature and thermal shock resistant container. Quartz was selected due to aforementioned reasons. The cell was placed into a quartz vessel of 5 cm inner diameter and 60 cm height. The quartz vessel was covered by a castermid lid that was specially designed to insulate the top of the cell. This lid was embodied four holes for gas inlet, gas outlet, anode and cathode. All of the holes were established with polymer O-rings to set up a system that was vertically adjustable without any gas leak.

3.1.1 Auxiliary Apparatus

The electrical power for the electrolysis was supplied via a programmable Plating Electronic pe86C pulse reverse DC power supply (PDC). Corresponding current values were observed by power supply and potential differences were recorded by Agilent U1273AX digital multimeter. Potential difference data were recorded as a function of time by Agilent GUI Data Logger software. The cell assembly was positioned into a programmable Lindberg LHTF3226 vertical split furnace. The heater elements of the furnace were made of Kanthal wires. Temperature measurements were made by a K type thermocouple.

The furnace was placed into a fume cupboard like cabin made of poly propylene (PP). The cabin was connected to an adjustable air suction system. Argon gas flow was supplied at a rate of 200 ml/minute to create an inert atmosphere in the cell vessel. In addition, gaseous products of the electrolysis were carried out by this gas flow. A photograph of the overall experimental setup is given in Figure 3.2.

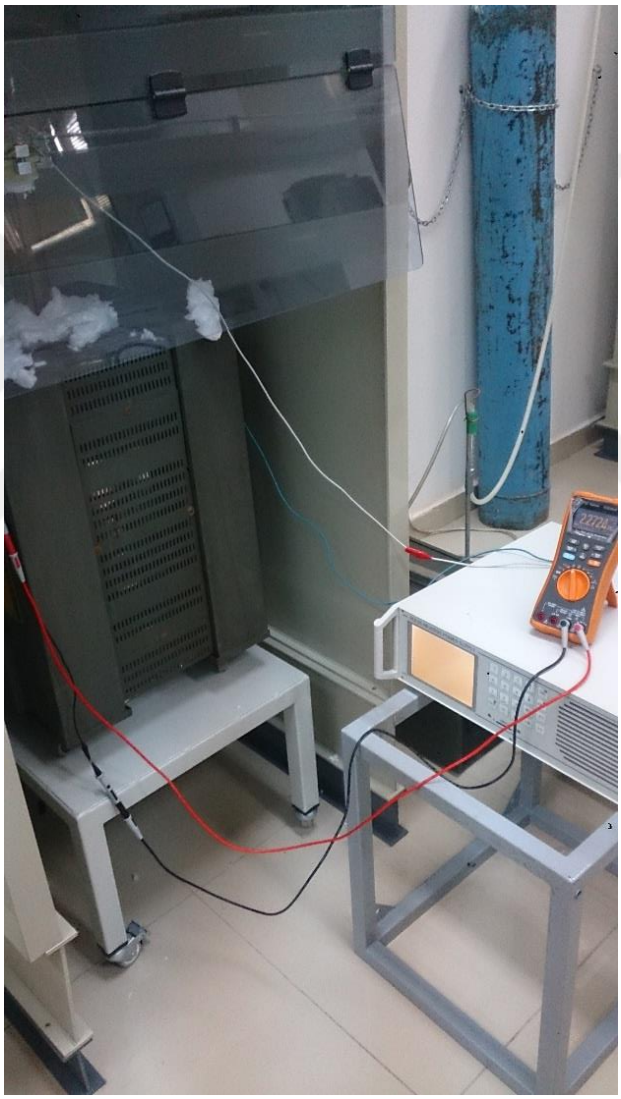


Figure 3.2 A photograph of the overall experimental setup

3.1.2 Cell Feed Preparation

2.5 gram of $CaWO_4$ (Aldrich 24,866) powder was dry pressed under 2 tons of load to form a pellet. Water was used as binder where the dry pressing of powder was not sufficient to form a pellet. The pellets were dried in an oven at 130^{o}C to remove the water that was used as binder.

The electrolyte was a molten solution of calcium chloride and sodium chloride salts at eutectic point (48%mol NaCl at 873 K, see Figure 3.3.). Both salts were dried to obtain anhydrous oxide free electrolyte. $CaCl_2$ was dried extensively to remove the possible presence of physically and chemically bounded moisture.

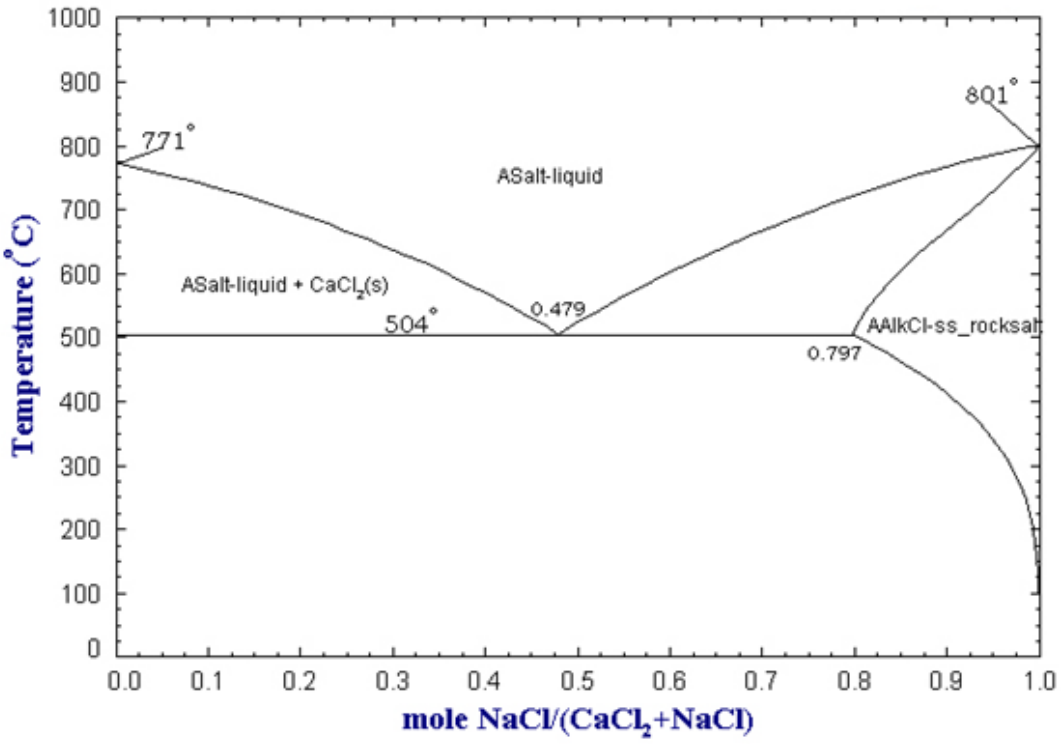


Figure 3.3 Phase diagram of the $CaCl_2$-NaCl system. Reproduced from [44]

The phase diagram for $CaCl_2$-H_2O system is given in Figure 3.4. Referencing Figure 3.4, it can be stated that oxide free anhydrous $CaCl_2$ could be obtained via close control during drying. $CaCl_2$ was first heated to 110°C and held for three hours. Then the temperature was ramped to 550°C with a rate of 1°C/min and held for 24 hours. All of the drying procedure was conducted under vacuum to remove chemically bounded moisture and minimize oxide formation. On the other hand, NaCl was heated to 130°C and held at this temperature for 24 hours.

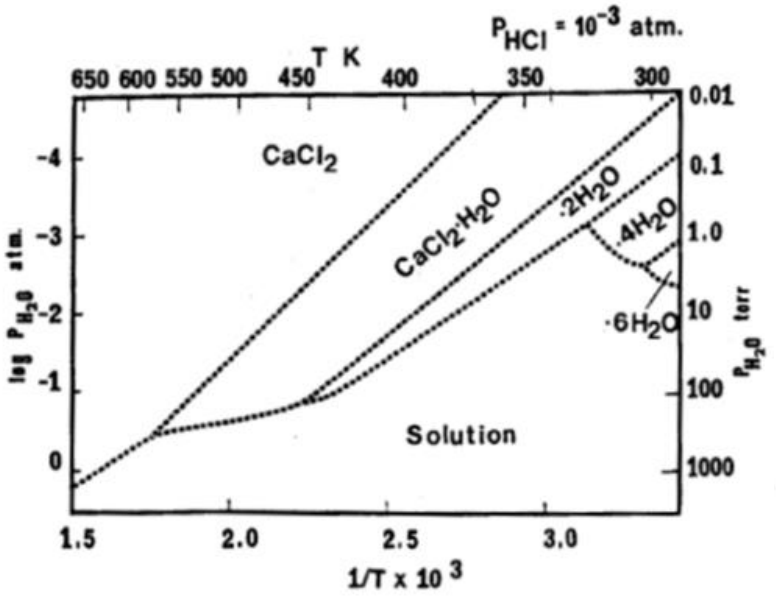


Figure 3.4 Phase diagram of $CaCl_2$-H_2O system. Reproduced from [45].

Electrolyte was made of approximately 28.1 grams of NaCl and 57.7 grams of $CaCl_2$. Electrolyte was placed into an alumina crucible which was placed into a quartz vessel after mixing the salts. Subsequently, all the other auxiliary apparatus were placed and heating process was started. Heating rate was selected as 1°C/min in order to get rid of any residual moisture. In addition, argon gas flow was provided both in heating and also during the whole experiment duration. Hereupon, target temperature was selected as 600°C that provided molten state of the electrolyte as it can be seen from Figure 3.3. After the time given for electrolyte to stabilize and homogenize, the

electrodes were lowered and plunged into the molten electrolyte. Then the PDC power supply and multimeter attachments were introduced to the electrodes.

3.1.3 Pulse Current Parameters

Tungsten production by the electrochemical reduction method was stated as energy efficient in the previous studies [34, 47]. Therefore, electrochemical method has the potential to decrease energy consumption in tungsten production. Moreover, electrochemical reduction of $CaWO_4$ by pulse potential was reported to have further flexibility to influence electrode processes [47], because it is known that pulse current electroplating improves mass transport, electrode kinetics and the nucleation of growth centers [49, 50]. Therefore, a set of experiments was designed for the pulse current electrochemical reduction of $CaWO_4$. Average current, pulse on and pulse off durations were selected as variables. The values of parameters used in this study are given in the Table 3.1.

Table 3.1 Experimental Parameters

Average Current (A)	**I_{peak} (A)**	**t_{on} (ms)**	**t_{off} (ms)**
0.1	0.5	1	4
0.1	1	1	9
0.1	2	1	19
0.1	0.2	1	1
0.2	1	1	4
0.2	2	1	9
0.2	4	1	19
0.2	0.4	1	1
0.3	1.5	1	4
0.3	3	1	9
0.3	6	1	19
0.3	0.6	1	1

The corresponding voltage values were not allowed to excess 3.2 V. This value was set in order not to allow decomposition of the salts used in the molten salt medium (E^o_{CaCl2}= -3.4 V, E^o_{NaCl}=-3.37 V).

Average current values were calculated according to following equation,

$$I_{avg} = \frac{I_{peak} \times t_{on}}{t_{on} + t_{off}} \tag{2.16}$$

where I is average current, I_{peak} is the peak current, t_{on} and t_{off} are the pulse and relaxation durations in milliseconds respectively.

The relaxation durations were varied as 1, 4, 9 and 19 ms at 1 ms constant pulse duration. The frequency (f) and duty cycle (Θ) can be calculated according to following equations;

$$\Theta(unitless) = \frac{t_{on}}{t_{on} + t_{off}} \tag{2.17}$$

$$f(\frac{1}{\text{sec}}) = \frac{1}{t_{on} + t_{off}} \tag{2.18}$$

3.2 Large Scale Experiments

A pilot scale system was designed with a tungsten production capacity of approximately 300 grams per day. The external dimensions of the furnace were 500 mm diameter and 500 mm height. Furnace had three rows of Kanthal resistance wires at the side walls and one row at the bottom. By this way, it became possible to heat the furnace by the resistances positioned at the side walls or at the bottom alone or using both of the resistances. The furnace was located in a fume cupboard like cabin which was made of polypropylene (PP). The cabin was connected to an adjustable air suction system to collect gaseous products of the reactions.

3.2.1 Cell Feed Preparation of Large Scale Experiments

A stainless steel (AISI 316Ti) vessel was placed into the furnace to contain the molten salt. It had 360 mm outer diameter, 4 mm thickness and 360 mm height. The $CaWO_4$ (Noah, 18418) powder was introduced to the molten salt within a stainless steel (AISI 316Ti) current collector as the target temperature of 600^oC was reached.

Graphite was used as the anode material. Different modifications were applied to the graphite rods. As it can be seen from Figure 3.5, one of the graphite rods was surrounded with Al_2O_3 in the outer sections to prevent the contact of graphite and molten salt medium.



Figure 3.5 A photograph of the system and alumina coated graphite

Also, boron nitride coating was applied on another graphite surface. The coated graphite rods had treads for the attachments of the uncoated contact parts of graphite that had larger-diameters. In order to be able to modify the position of the graphite rod vertically, an elevator system was placed next to the furnace. The system was composed of a supporting arm to keep the graphite anode at the center of the furnace, a rotating screw and an insulator system placed into a U profile. An AC electric motor and a redactor were used to rotate the screw at low speed to move the anode in the up and down directions. The system carrying the arm was insulated with the help of a castermid insulator in order to supply electrical current directly to anode material. A photograph of the complete large scale tungsten production system used in this study can be seen in Figure 3.6.



Figure 3.6 A photograph of the complete system

The electrolyte for the large scale tungsten production was prepared by using technical grade salts unlike the reagent grades used in the laboratory scale experiments. They were selected to associate the process for possible industrialization in future. For this purpose; hydrated $CaCl_2$ (Solvay) and NaCl (Ucleroglu) salts were mixed to obtain a salt solution of eutectic composition as the electrolyte.

Melting of the salt mixture was completed in 48 hours pursuant to extensive drying procedure. By this way, most of the H_2O that $CaCl_2$ contained was removed at low temperatures. Furnace was programmed to reach 110^oC at a rate of 1^oC/min and held there for 12 hours. Then the temperature was ramped to 500^oC at a rate of 1^oC/min and held there for 24 hours.

Subsequently, melting was completed at the target temperature of 600 ^oC. Argon gas flow was provided during both heating steps to aid dehydration and the electrolysis.

In the experiments, about 20 kg of salt mixture consisting of 12.77 kg $CaCl_2$ and 7.23 kg NaCl (balance H_2O) was placed into the bath so as to provide 10 cm electrolyte depth. The $CaCl_2$ salt contained 2 moles of H_2O per mole so that 17 kg of $CaCl_2.2H_2O$ was used at the beginning to achieve 12.77 kg of $CaCl_2$. The $CaCl_2$ was dehydrated after 4.16 kg of H_2O was removed during heating.

$CaWO_4$ (Noah, 18418) powder was used in the experiments. EDS analysis of the powder is given in Table 3.2. As it can be seen from this table, the powder contains about 1.4 % wt. Na which was probably caused by the soda roasting and leaching step of $CaWO_4$ production [17]. Presence of sodium is not desired due to formation of bubbles when it was introduced to molten salt. Therefore, $CaWO_4$ powder was washed in a 0.1 M HCl solution to eliminate sodium present in the powder. The $CaWO_4$ powder, weighing 100 gr, was placed onto the stainless steel cathode current collector and dipped into the electrolyte, as temperature reached to the target temperature of 600 ^oC.

The graphite rod was also dipped into the electrolyte and the process was initiated by application of a potential difference of 2.8 to 3 V between the cathode and the anode. The electrical power was supplied via Agilent N6700B DC power supply. The current versus time data were recorded via a self-developed computer software. The experiments were carried out for 8 to 18 hours.

Table 3.2 EDS analysis of the $CaWO_4$ (Noah, 18418) powder.

Element	Wt. %	At %	K-Ratio	Z	A	F
C K	4.11	13.78	0.0101	1.1600	0.2111	1.0003
O K	22.55	56.79	0.0106	1.1432	0.1430	1.0000
Na K	1.42	2.45	0.0032	1.0730	0.2133	1.0002
Ca K	14.31	14.37	0.0818	1.1115	0.5113	1.0052
W L	57.61	12.61	0.5107	0.8434	1.0511	1.0000
Total	100	100				

3.3 Post Electrolysis Work

Argon gas flow was continued to supply during cooling of the cell. The samples contained the reduced part together with the solidified salts from the electrolyte. The collected samples were left into the deionized (DI) water to dissolve salts and separate the reduced parts. The samples were collected via filter paper (S&H Labware) for characterization. Samples were cleaned with dilute HCl solution to eliminate calcium byproducts as suggested in the previous studies [3, 35]. The reduced samples were washed with 0.2 M 600 ml of HCl solution in glass beakers and samples were obtained for further characterization.

3.3.1 Characterization

Raw materials, intermediate and final product samples of laboratory and large scale experiments were characterized via scanning electron microscope (FEI Nova NanoSEM 430), and X-ray diffractometer (Rigaku D/Max2200/PC). CuKα radiation was used in Rigaku diffractometer for XRD analyses. Data were obtained with a scan rate of 1°/min and sampling width of 0.02°. X-ray data were refined by the Rigaku qualitative analysis software.

Elemental analyses were performed by the use of an energy dispersive system (EDS) which was attached to Nova NanoSEM 430 scanning electron microscope.

CHAPTER 4

RESULTS AND DISCUSSION

4.1 Laboratory Scale Experiments

The laboratory scale experiments in this study were performed under pulse current conditions. By this way, the production of tungsten refractory metal powders by pulse current reduction of $CaWO_4$ in $CaCl_2$-NaCl electrolyte at 600 ^oC was investigated. The effects of applied current and its waveform on the reduction yield, energy consumption and shape and size of the produced powder were analyzed by setting average current, peak current and pulse and relaxation times as the parameters.

4.1.1 Determination of Current Parameters

The mechanism of the reduction of $CaWO_4$ was analyzed to determine the average current values that will be used for pulse current experiments. Constant voltage and constant current experiments by Erdoğan [17] already indicated the theoretical potential for the electrochemical reduction of $CaWO_4$. It was stated that the theoretical minimum potential for the reduction of $CaWO_4$ should be 2.25 V [50]. To be able to compare direct current and pulse current results and derive conclusions on the effects of pulse current applications, 0.1, 0.2 and 0.3 A were selected as average current values for pulse current experiments similar to the previous study [50].

4.1.2 Experiments by Pulse Current

Applied pulse current generated a corresponding potential difference that was recorded during experiments. The recorded potential values as a function of time can be seen for tests employing 0.3 A average current in Figure 4.1.

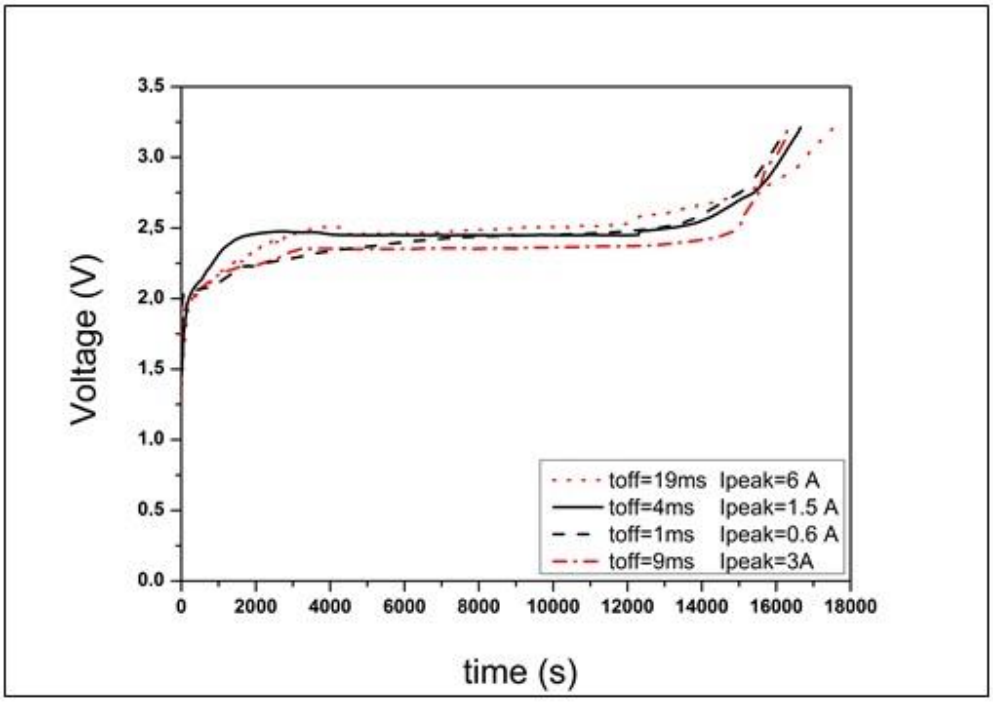


Figure 4.1 Voltage vs. time graphs for 0.3 A average current

The recorded potential values as a function of accumulative electrical charge passing through the system can be seen for tests employing 0.2 and 0.3 A average current values in Figure 4.2. Electrical charge was used in the presentation of the data to express the results more clearly and compare the level of reduction in different experiments. The accumulative electrical charge, Q, is given by; Eq 2.19.

$$Q = \int_0^t Idt \tag{2.19}$$

Where, Q is the charge in coulomb, I is the current in ampere and t is the time for second.

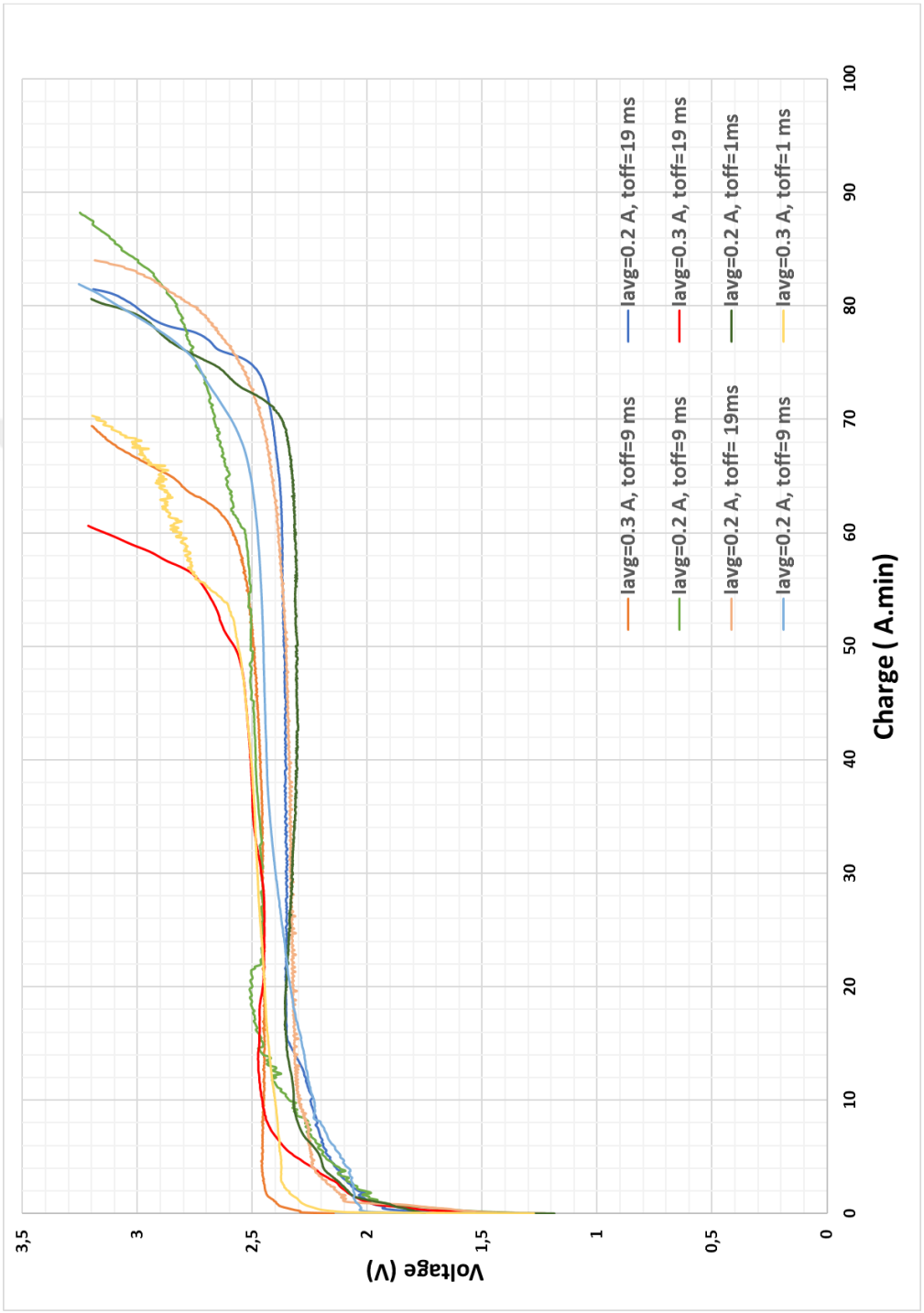


Figure 4.2 Voltage as a function of charge (A.min) for the selected experiments

Since the raw materials were identical in size and geometry in all experiments, current density calculations were not needed and the recorded voltage values were directly comparable. The behavior of all the recorded curves were similar to each other and to those recorded during constant current reduction experiments [50]. Voltage values started with a minimum and increased as time passed. The values showed a rapid increase in the initial stages for all experiments and the increase continued up to a level where formation of a plateau was observed. The starting values of the voltages were between 1 and 2.2 V depending on the current values. The starting voltage values can be better analyzed from Figure 4.3 and Figure 4.4 in which first ten minutes of the plots were redrawn for tests employing 0.1 and 0.2 A average current values.

The initial voltage increase can be attributed to the resistance of the pellet. At the beginning of the process, the three phases; the Kanthal wire current collector, the pellet and the molten salt, were in contact with each other. As the reduction starts from this three phase interface, the pellet resistance was not important and the corresponding voltage values were lower at the start of the experiments for a short while. However, just after metallization of the surface with a thin layer of tungsten, the contact between the $CaWO_4$ pellet and the electrolyte was lost and the pellet resistance became more pronounced. There are plateaus formed in each of the experiments subsequent to this rapid voltage increase (See Figures 4.1-4.5). The plateaus indicated the presence of steady state conditions in the reduction processes. The second increase was considered as the finalization of the ongoing reduction and increase in pellet resistance. Further increase in potentials may initiate the decomposition of $CaCl_2$. Therefore, the power supply was switched off as the potential difference value reached to 3.2 V.

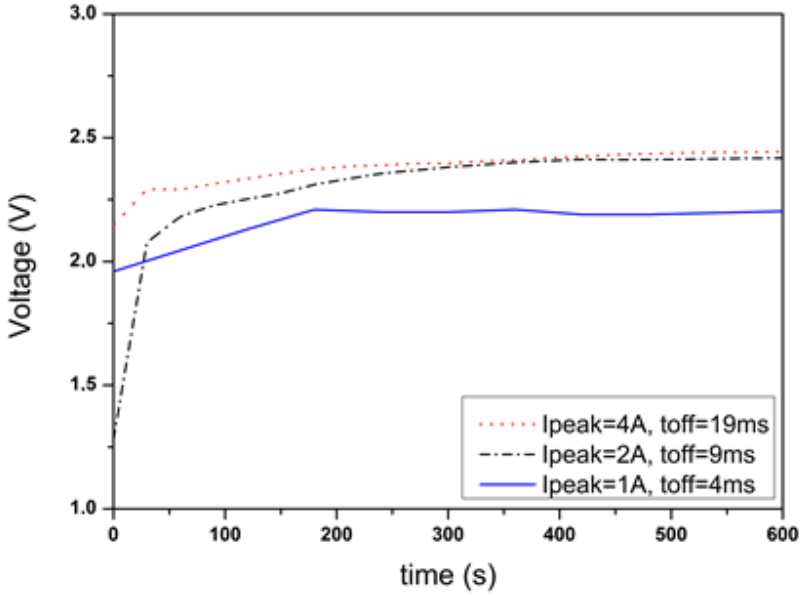


Figure 4.3 Potential values as a function of time for the first ten minutes of the experiments with 0.2 A average current

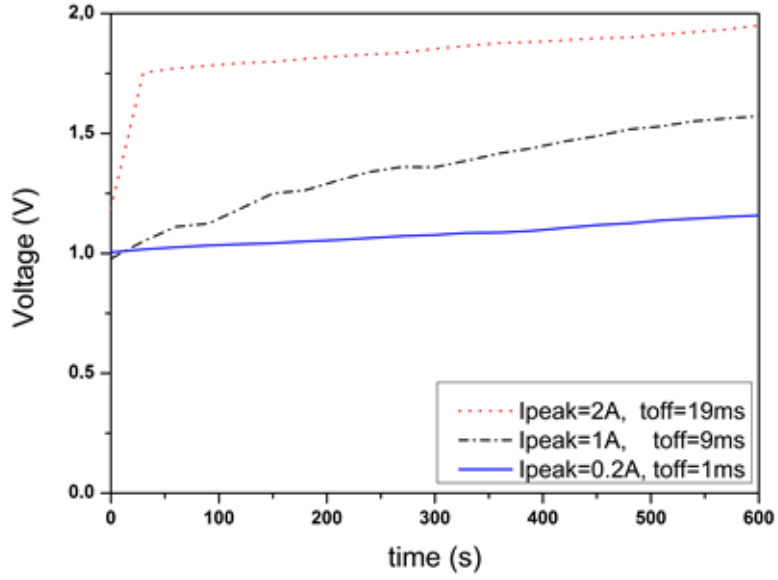


Figure 4.4 Potential values as a function of time for the first ten minutes of the experiments with 0.1 A average current

The effect of the average current can be clearly seen in the experiments conducted by fixed pulse duration (t_{off}=9 ms) given in Figure 4.5. It can be seen from Figure 4.5 that increasing the average current value leads to a decrease in the overall time required for reduction. Theoretically, this phenomenon can be explained by Faraday's first law of the electrolysis by the equations:

$$Q \times A \times CE = W \times z \times F \tag{2.20}$$

Where Q is the charge in coulombs, A is the molecular weight of the $CaWO_4$, W is the theoretical amount of reduction, z is the valance number, F is the constant of Faraday (96485 $C.mol^{-1}$) and CE is the current efficiency.

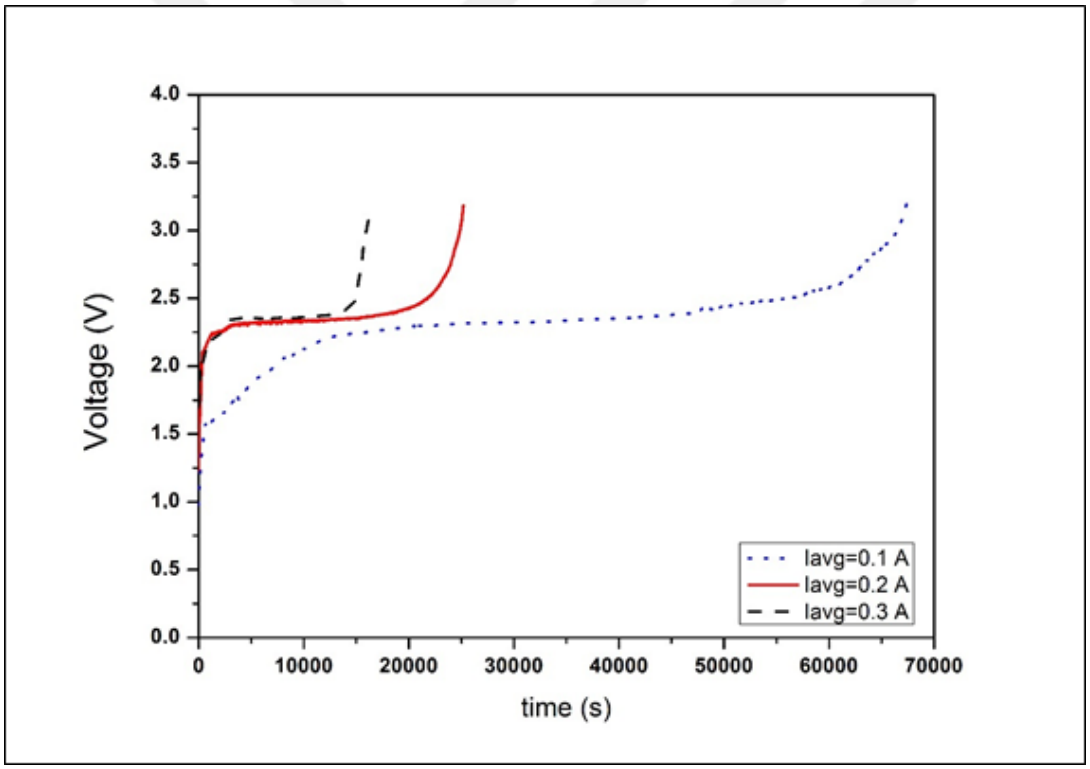


Figure 4.5 Voltage as a function of time for the experiments performed with 0.1, 0.2 and 0.3 A average current and fixed pulse relaxation time at 9 ms

Theoretical charge required for the reduction of 2.5 grams of $CaWO_4$ is 5026.75 Coulombs. Since the charge is the product of current and time, replacing "*I*" with average current in equation 2.19 and reorganization for the time provides the time required for the complete reduction assuming 100% current efficiency as suggested by equation 2.19.

2400 coulombs of charge is required for about 48 wt.% theoretical reduction of 2.5 g $CaWO_4$. This value was selected to be able to compare the results with DC experiments that the potential values for the passage of the 2400 C of charge through the system are already reported [50]. The passage of 2400 C corresponds to 24000 seconds for 0.1 A, 12000 seconds for 0.2 A and 8000 seconds for 0.3 A average current. The corresponding average voltage values for these parameters can be seen in Table 4.1.

Table 4.1 Corresponding average potential values for 48wt% theoretical reduction of $CaWO_4$

Average Current	**t_{off}=0* (DC)**	**t_{off}=1 ms**	**t_{off}=4 ms**	**t_{off}=9 ms**	**t_{off}=19 ms**	**Corresponding time (s)**
0.1 A	2.35	2.25 V	2.22 V	2.30 V	2.31 V	24000
0.2 A	2.55	2.40 V	2.34 V	2.44 V	2.47 V	12000
0.3 A	2.70	2.43 V	2.35 V	2.42 V	2.49 V	8000

*Values are taken from [50]

As it can be seen in Table 4.1, all the voltage values recorded for pulse current experiments were lower than those for DC experiments when the average current values were the same. The values decreased up to t_{off} =4 ms and then started to increase but did not reach the level recorded for DC experiments within the parameter range covered in this study. The decrease in voltage values was due to the modification of the electrode kinetics via pulse application to the current. The modification was more distinct in 0.3 A because electrode polarizations increase as current is increased for DC plating.

4.1.3 Properties of the Produced Powder

After switching off the power supply, the cell was left to cool down to room temperature in the furnace under argon gas flow. The anode and cathode assemblies were pulled up to a higher level than the electrolyte while the electrolyte was still liquid. The reduced pellet on the cathode part was covered with solidified salts. The cathode was left into water to dissolve the salts and to separate the produced powder. The solution was filtered after the complete dissolution of the salt. In addition, the solidified salt in the alumina crucible was dissolved and filtered. Finally, XRD analysis was conducted to examine powder products. Figure 4.6 indicates the XRD pattern of the reduced sample obtained from the experiment involving 0.2 A average current and 9 ms pulse relaxation time.

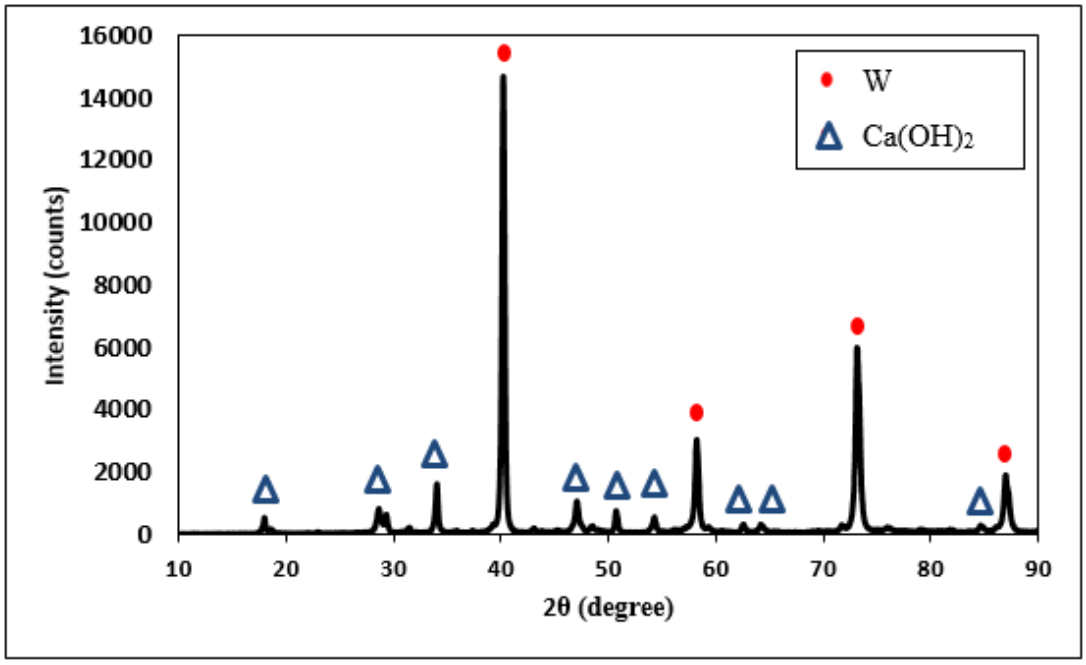


Figure 4.6 XRD result of the cathode sample, I_{avg}=0.2 A, t_{off}=9 ms

All of the XRD patterns of the produced powders indicated the characteristic peaks of tungsten. Besides, there were other peaks observed. As it can be seen from Figure 4.6, presence of $Ca(OH)_2$ was observed in all of the experiments as it was reported in previous studies [3, 48]. Presence of $Ca(OH)_2$ can be explained by the reaction of

water with calcium or calcium oxide which are possible products of the electrolysis. In addition, presence of $CaCO_3$ was observed in some of the XRD patterns of the experiments. Presence of $CaCO_3$ can be explained as a byproduct formation of calcium oxide and carbon dioxide (CO_2). This formation was a result of insufficient argon gas flushing especially when the current was not applied. The experiments with argon gas supply including the cooling period after the electrolysis indicated presence of no $CaCO_3$.

The solidified electrolyte was also dissolved in water and filtrated for further characterization. The presence of tungsten was detected in the XRD patterns of the samples obtained from the solidified electrolyte as it can be seen from Figure 4.7.

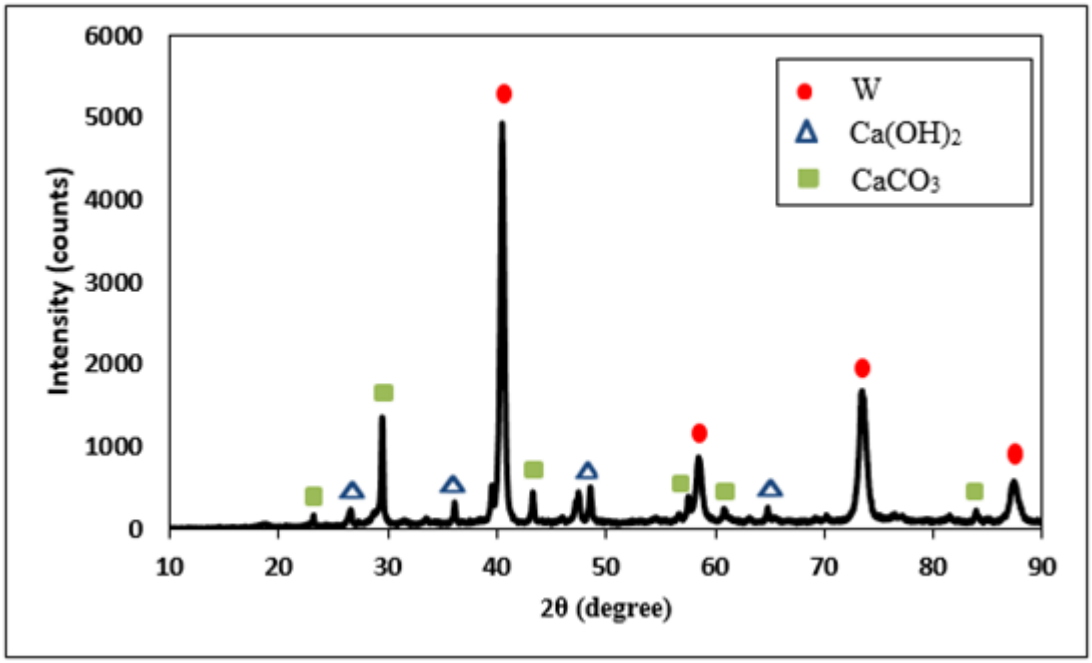


Figure 4.7 XRD result of the sample obtained from electrolyte, I_{avg}=0.2 A, t_{off}= 19 ms

The samples collected from the cathode and the electrolyte were directed to a cleaning process to separate metallic tungsten powder and remove calcium by products. This process was conducted by introducing the samples into a dilute hydrochloric acid solution. 0.2 M 600 ml HCl solution was prepared and stirred via magnetic stirrer to dissolve the byproducts. Characterization results indicated that

tungsten was inert enough in such a solution and byproducts of calcium were completely removed.

Figure 4.8 indicates the X-ray diffraction result of a sample which was cleaned with 0.2 M HCl solution. As it can be seen in this figure, the only remained peaks were belonging to tungsten and there were no calcium byproducts detected in the pattern. All of the samples cleaned with 0.2 M HCl solution indicated similar X-ray diffraction patterns to the one presented in Figure 4.8.

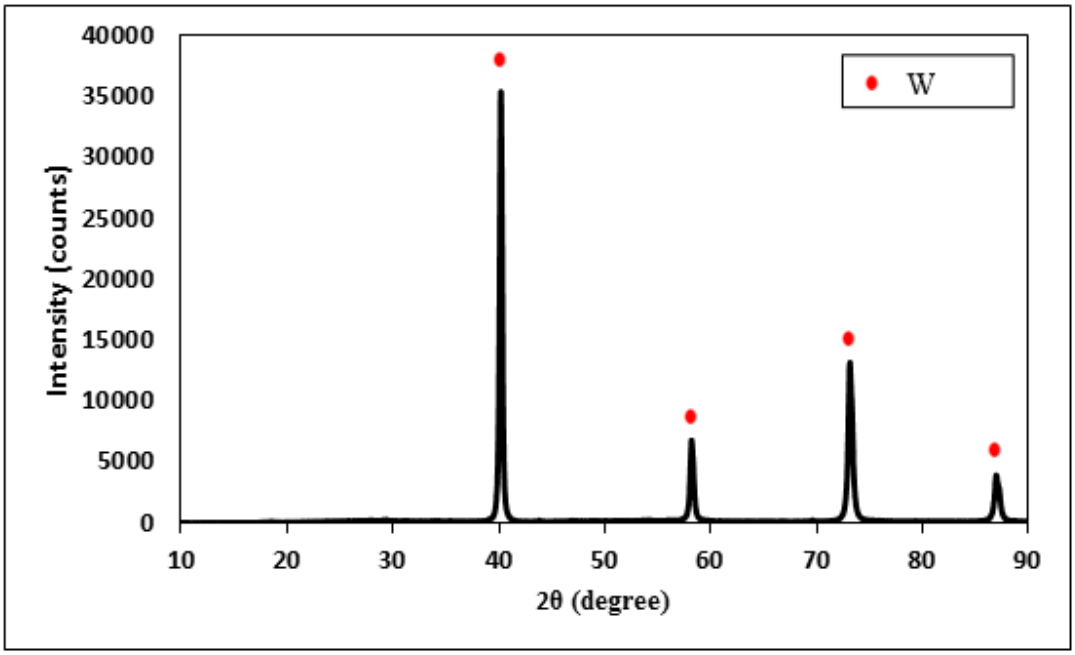


Figure 4.8 X-ray diffraction pattern of a sample cleaned with 0.2 M HCl solution, I_{avg}=0.3 A, t_{off}=9 ms

Further characterization was required to determine the size and shape of the produced powders. SEM photographs of the raw material and final product are given in Figure 4.9 and Figure 4.10. As it can be seen in Figure 4.9, most of the particle size of the starting pellet was less than 10 μm. Figure 4.10 indicated that particle size determination was very difficult because of the agglomeration of particles and necking between grains. However, it is possible to deduce that produced powder was comprised of agglomerated nano-scale particles when carefully examined.

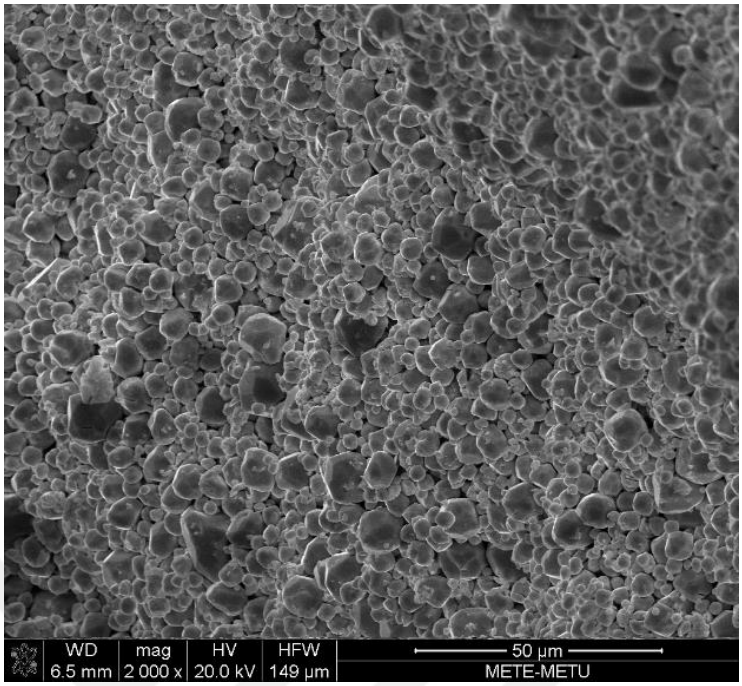


Figure 4.9 SEM photograph of the raw material pellet ($CaWO_4$)

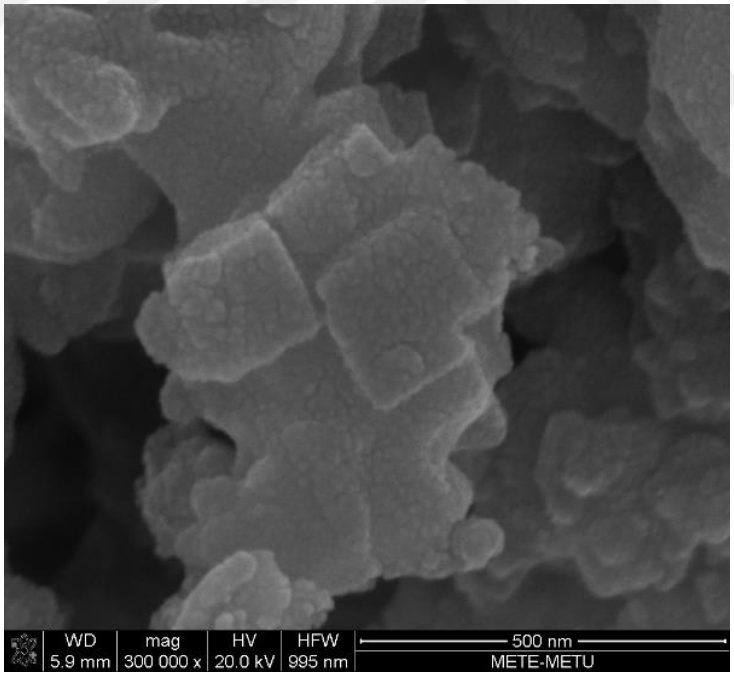


Figure 4.10 SEM photograph of the reduced powder I_{avg}=0.3 A, t_{off}=19 ms

The SEM photographs of some of the experiments that were conducted using different average currents and pulse relaxation times are shown in Figure 4.11. As it

can be seen in this figure (Figure 4.11-d), some of the samples indicated whisker-like structures together with spherical particles.

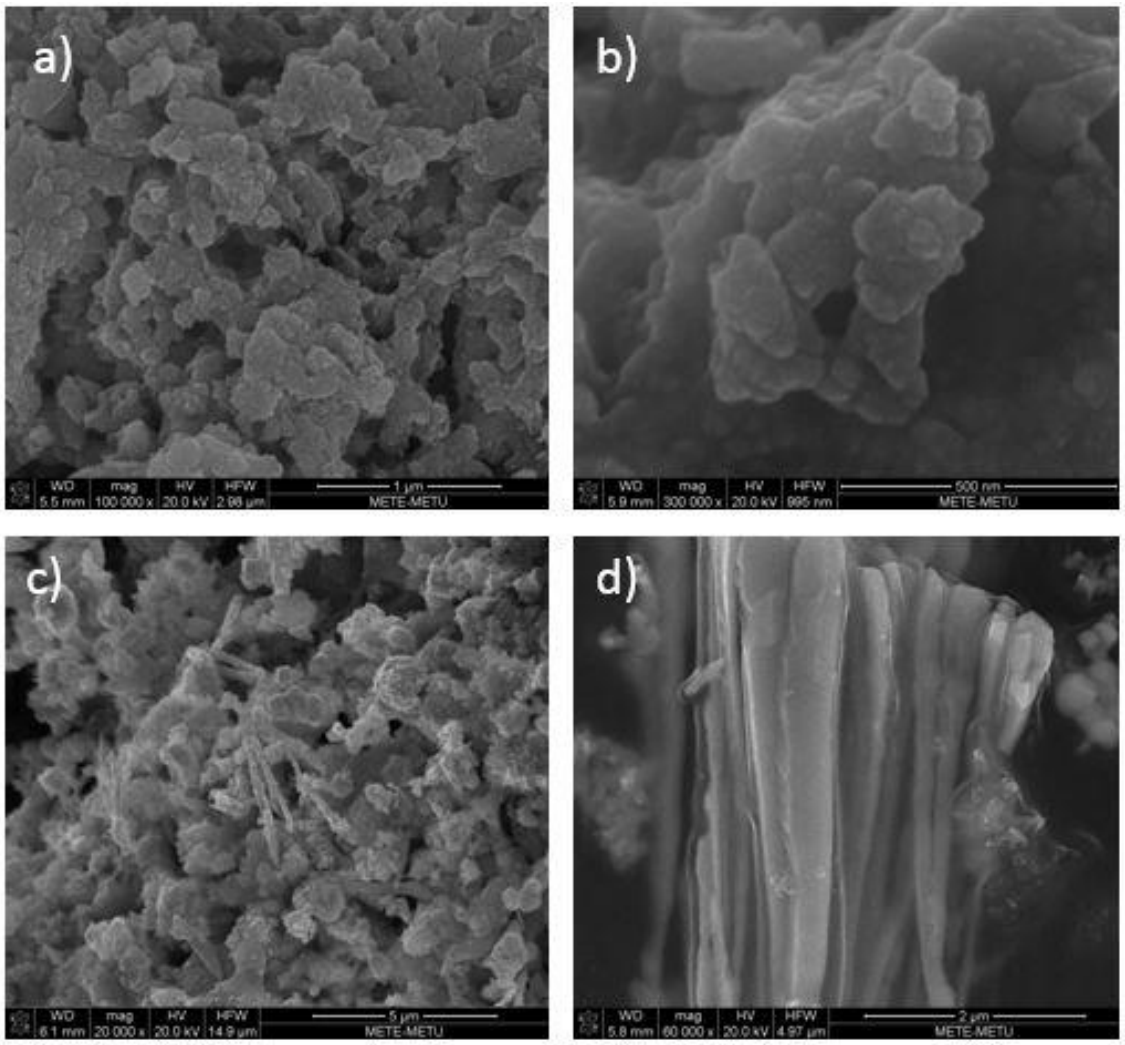
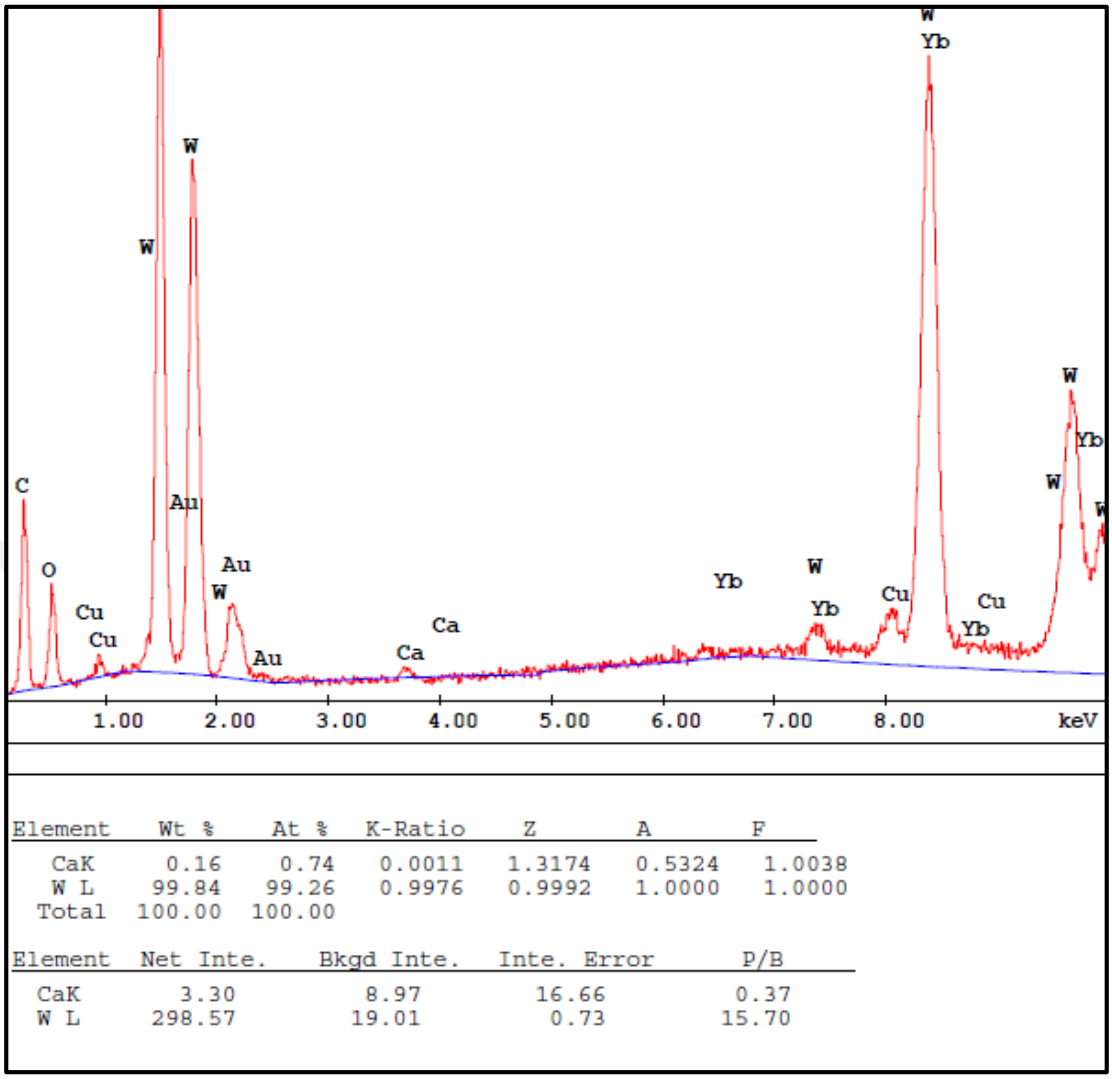


Figure 4.11 SEM photographs of the samples produced with a-) I_{avg}=0.3 A, t_{off}=19ms b-) I_{avg}=0.2 A, t_{off}=9 ms c-) I_{avg}=0.3 A, t_{off}=1ms d-) I_{avg}=0.2 A, t_{off}=1ms

EDS analyses indicated that whiskers had almost the same composition as the spherical particles (See Figure 4.12). The formation of these shapes mostly observed in the samples that were produced when pulse relaxation time was 1 ms. It was considered that pulse parameters affected the final particle shape.



Element	Wt %	At %	K-Ratio	Z	A	F
CaK	0.16	0.74	0.0011	1.3174	0.5324	1.0038
W L	99.84	99.26	0.9976	0.9992	1.0000	1.0000
Total	100.00	100.00				

Element	Net Inte.	Bkgd Inte.	Inte. Error	P/B
CaK	3.30	8.97	16.66	0.37
W L	298.57	19.01	0.73	15.70

Figure 4.12 EDS analysis of the lath shaped particles obtained from I_{avg}=0.2 A, t_{off}=1ms

The peak intensities of the X-ray diffraction analysis of these samples were presented in Table 4.2. In addition, X-ray diffraction analysis of a commercially available tungsten powder was conducted and relative intensity values for the crystallographic planes were presented in Table 4.2 for comparison.

Table 4.2 Relative intensity values for the crystallographic planes of the samples from this study and commercial tungsten powder

Iavg=0.2 A toff=9ms

C.Plane	R.Intensity
(110)	100
(200)	22
(211)	40
(220)	13

Iavg=0.3 A toff=9 ms

C.Plane	R.Intensity
(110)	100
(200)	20
(211)	38
(220)	12

Iavg=0.3 A toff=19 ms

C.Plane	R.Intensity
(110)	100
(200)	23
(211)	38
(220)	14

Iavg=0.2 A toff=1 ms

C.Plane	R.Intensity
(110)	100
(200)	15
(211)	23
(220)	7

Iavg=0.1 A toff=1 ms

C.Plane	R.Intensity
(110)	100
(200)	14
(211)	23
(220)	7

Commercial W powder

C.Plane	R.Intensity
(110)	100
(200)	17
(211)	33
(220)	10

The percentage distributions of relative intensities of four detected peaks are presented in Table 4.3. Comparison of the percent relative intensity values for the crystallographic planes indicated that the growth of crystal was favored more in the (110) plane for the experiments conducted at 1 ms pulse relaxation time relative to others. On the other hand, growth favored more in (211) plane as the pulse relaxation duration increased. Nevertheless, direct comparison of the pulse relaxation times could not be considered due to different peak current values in the experiments.

Table 4.3 Relative intensities as percentages between four detected peaks

Iavg=0.2 A toff=9ms

C.Plane	R.Intensity
(110)	57.14
(200)	12.57
(211)	22.85
(220)	7.43

Iavg=0.3 A toff=9 ms

C.Plane	R.Intensity
(110)	58.85
(200)	11.75
(211)	22.35
(220)	7.05

Iavg=0.3 A toff=19 ms

C.Plane	R.Intensity
(110)	57.15
(200)	13.15
(211)	21.7
(220)	8

Iavg=0.2 A toff=1 ms

C.Plane	R.Intensity
(110)	68.95
(200)	10.35
(211)	15.85
(220)	4.85

Iavg=0.2 A toff=1 ms

C.Plane	R.Intensity
(110)	69.44
(200)	9.72
(211)	15.97
(220)	4.87

Commercial W powder

C.Plane	R.Intensity
(110)	62.5
(200)	10.62
(211)	20.62
(220)	6.25

4.1.4 Energy Consumption of the Pulse Current Experiments

Energy consumption is critical when industrial and environmental concerns are taken into consideration. In metal production industry, energy consumption is an important outcome for the electrochemical production of metals. Therefore, energy consumptions of the pulse current experiments were calculated. The calculations were based on the stoichiometric amount of tungsten produced after each experiment. Multiple EDS analyses on various parts of powders were conducted to determine the tungsten percentage of the produced powder.

The accumulative total charge passing through the system was calculated from the Eq. 2.21 when 100% current efficiency was assumed.

$$Q = \int_0^t I dt = \frac{100\ W\ z\ F}{A} \tag{2.21}$$

The recorded potential values as a function of time data were used to determine the energy consumption (ε) for each experiment.

$$\varepsilon = \int_0^t I * V\ dt \tag{2.22}$$

The amount of tungsten collected after each experiment, m, and the energy consumption, ε, were taken into consideration to calculate the electrical energy required per kilogram of tungsten production (E per kg W).

$$E(per\ kg\ W) = \frac{1000}{m} x\ \varepsilon \tag{2.23}$$

The statistical analyses of the results are presented in Table 4.4. The columns of, t_{off}, I_{avg} and number of tests for each parameter, N, are given in the table. Profile plots for the variables and binary interaction plots are given in Figure 4.14 and Figure 4.15 respectively.

Calculations indicated the energy consumption values were between 2.0 and 2.9 kWh per kg. These values are lower than the reported values (10.63 kWh per kg W, 4.96 kWh per kg W) for the energy required to produce one kilogram of tungsten via constant voltage experiments [34, 53]. Moreover, the values are lower than the ones required to produce aluminum (13.46 kWh per kg Al) [53] and magnesium (10.5-13.2 kWh per kg Mg) [54] which are most important metals produced via molten salt electrolysis.

Table 4.4 Descriptive statistics of energy consumption values

Descriptive Statistics			
Dependent Variable: Energy Consumption (kWh per kg W)			
t_{off}	I_{avg}	Mean	N
1	0.1	2.193	2
	0.2	2.193	2
	0.3	2.517	2
	Total	2.301	6
4	0.1	2.438	2
	0.2	2.202	2
	0.3	2.339	2
	Total	2.326	6
9	0.1	2.870	2
	0.2	2.329	3
	0.3	1.997	2
	Total	2.399	7
19	0.1	2.068	2
	0.2	2.019	2
	0.3	2.205	2
	Total	2.097	6
Total	0.1	2.392	8
	0.2	2.186	9
	0.3	2.265	8
	Total	2.281	25

As statistical results in Figure 4.13 showed, the highest energy consumption values were obtained from the experiments at 0.1 A average current value. This is considered as a result of holding the electrolysis longer than the theoretical duration to achieve complete reduction. Therefore, current efficiency was lower than the other experiments. The experiments at 0.2 and 0.3 A average current values indicated closer values. As the profile plots in Figure 4.14 show, the experiments involving 19 ms pulse relaxation time have the lowest mean for the energy consumption.

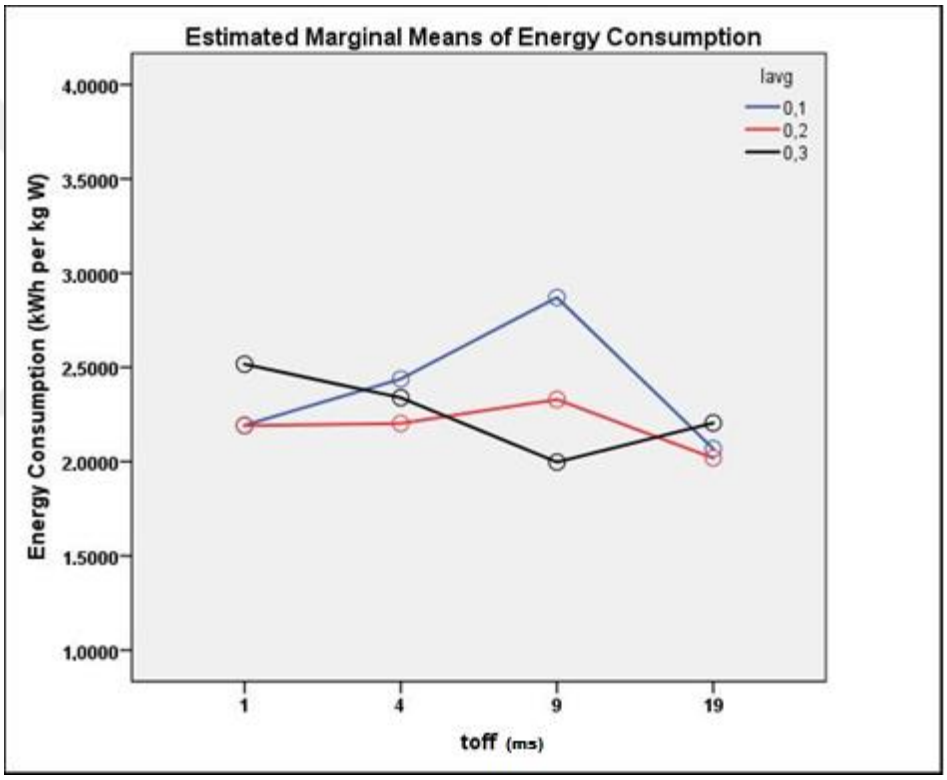


Figure 4.13 Estimated marginal means of energy consumption binary interaction plot

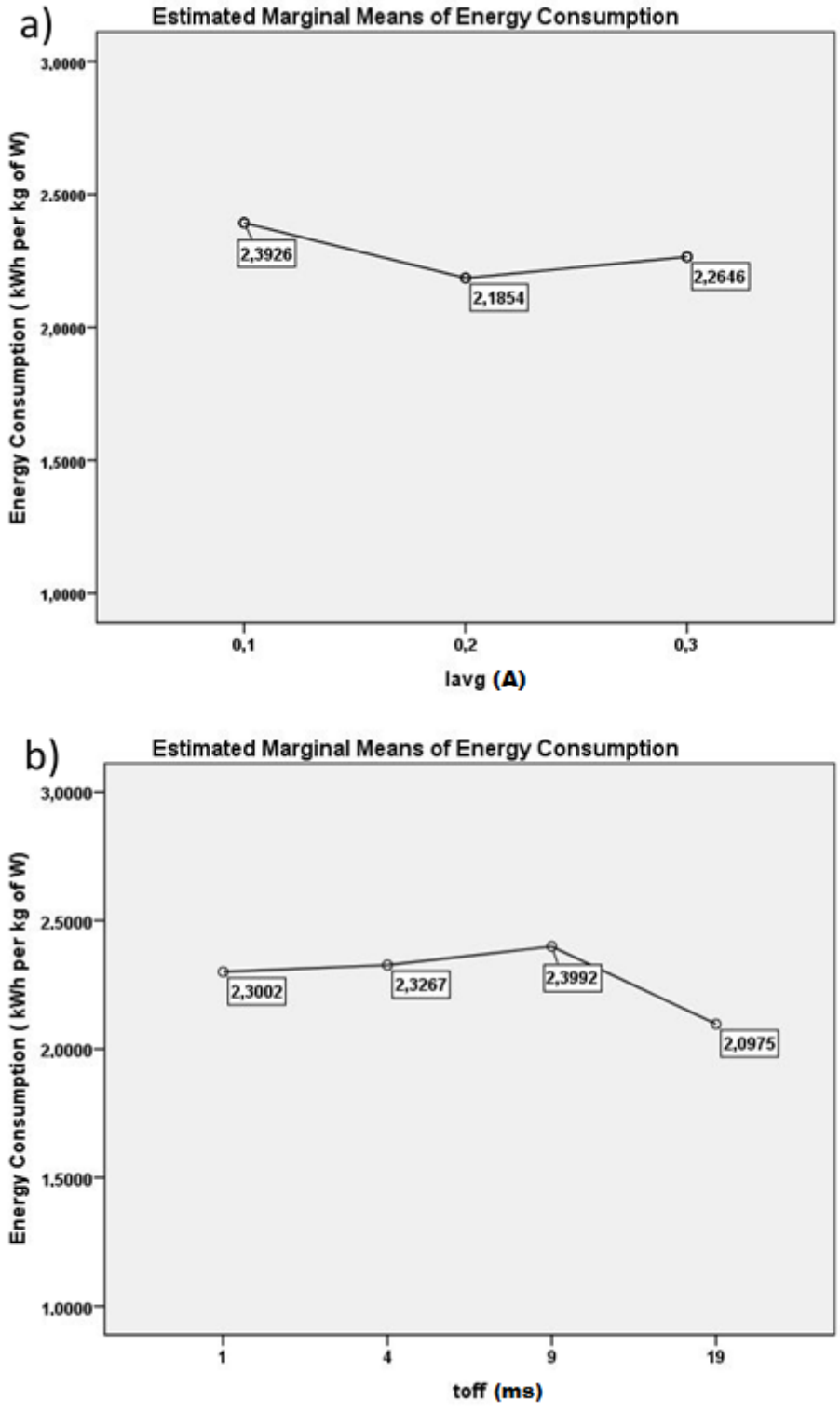


Figure 4.14 Profile plots for a) average current (I_{avg}) and b) pulse relaxation time (t_{off})

4.2 Large Scale Experiments

EDS analysis of the starting $CaWO_4$ powder (Noah, 18418) indicated the presence of sodium (Na) (See Table 3.2 in Chapter 3). Erdoğan already reported the presence of Na caused bubble formation when the raw material was introduced to the electrolyte at the reduction temperature. As a consequence, dispersion of the raw material into the molten salt was inevitable [17].

In order to eliminate the presence of Na, the $CaWO_4$ powder was subjected to a cleaning process via 0.1 M HCl solution. Subsequently, drying was applied in an oven at 200 ^oC. The EDS analysis of the cleaned $CaWO_4$ powder is presented in Table 4.5. Presence of Na was completely eliminated from the starting material. Cleaned $CaWO_4$ (Noah, 18418) powder was directly used in the experiments without pressing the powder unlike the ones used in the laboratory scale experiments.

Table 4.5 EDS analysis result of $CaWO_4$ powder after 0.1 M HCl cleaning

Element	**Wt %**	**At %**	**K-Ratio**	**Z**	**A**	**F**
C K	6.55	21.38	0.0163	1.1591	0.2148	1.0003
O K	21.72	53.06	0.0352	1.1424	0.1418	1.0000
Ca K	13.50	13.18	0.0775	1.1108	0.5140	1.0052
W L	58.21	12.38	0.5160	0.8429	1.0515	1.0000
Total	100	100				

In the light of findings from the laboratory scale experiments', powder product was subjected to a similar washing process to isolate the metallic powder. The solidified salt that was together with the reduced powder was dissolved in tap water to separate it from the cathode current collector. It was subsequently treated with 5 liters of a 0.2 M HCl solution for 30 minutes and a pulp was formed. The pulp was filtered under

vacuum and dried at room temperature to obtain the reduced powder. The XRD result of the product powder is given in Figure 4.15.

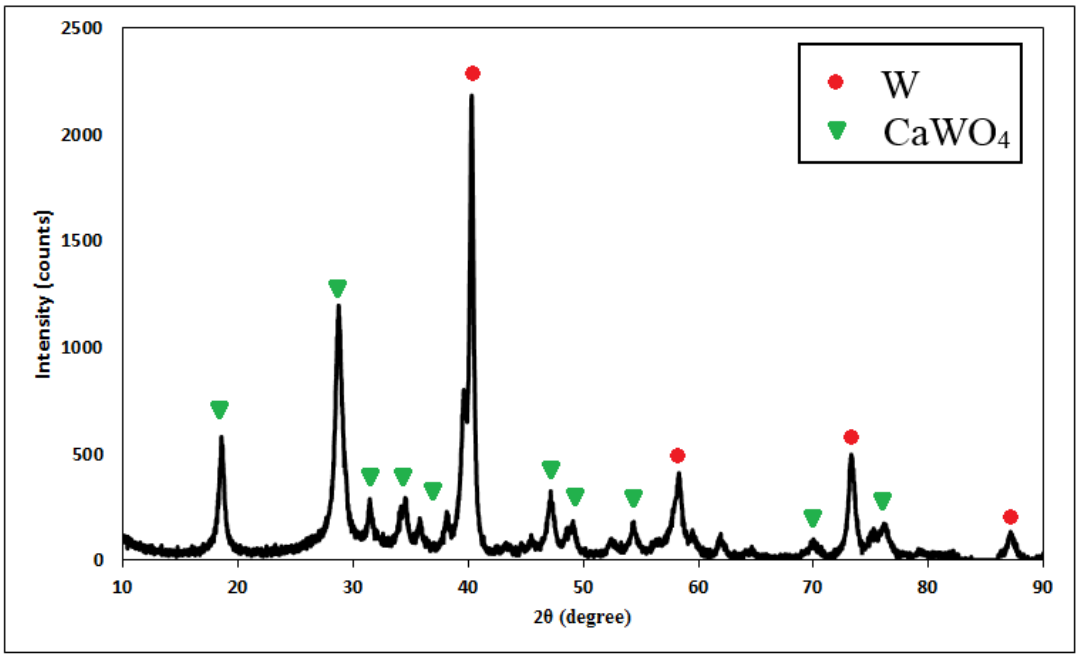


Figure 4.15 X-ray diffraction pattern of the produced and cleaned powder

As it can be seen in Figure 4.15, large scale production of tungsten was obtained via reduction of 60 grams of $CaWO_4$. However, reduction was not completely achieved. The incomplete reduction was also inferred from the plot of current as a function of time. The recorded current values, as a function of time is given in Figure 4.16. Theoretically, 120673 coulombs of charge is required to reduce 60 grams of $CaWO_4$. The charge that passed through the cell was two times more than required for complete reduction, yet the cell was still using current for reduction.

The problem most probably arisen due to the oxidation of graphite anode inside the furnace above the electrolyte level. As a consequence, graphite powders were dispersed in the molten salt and caused electronic conduction. Also, the rate of electrochemical reduction could not produce a large volume of carbon dioxide to enable sufficient positive pressure inside the cell to prevent air penetration into the system.

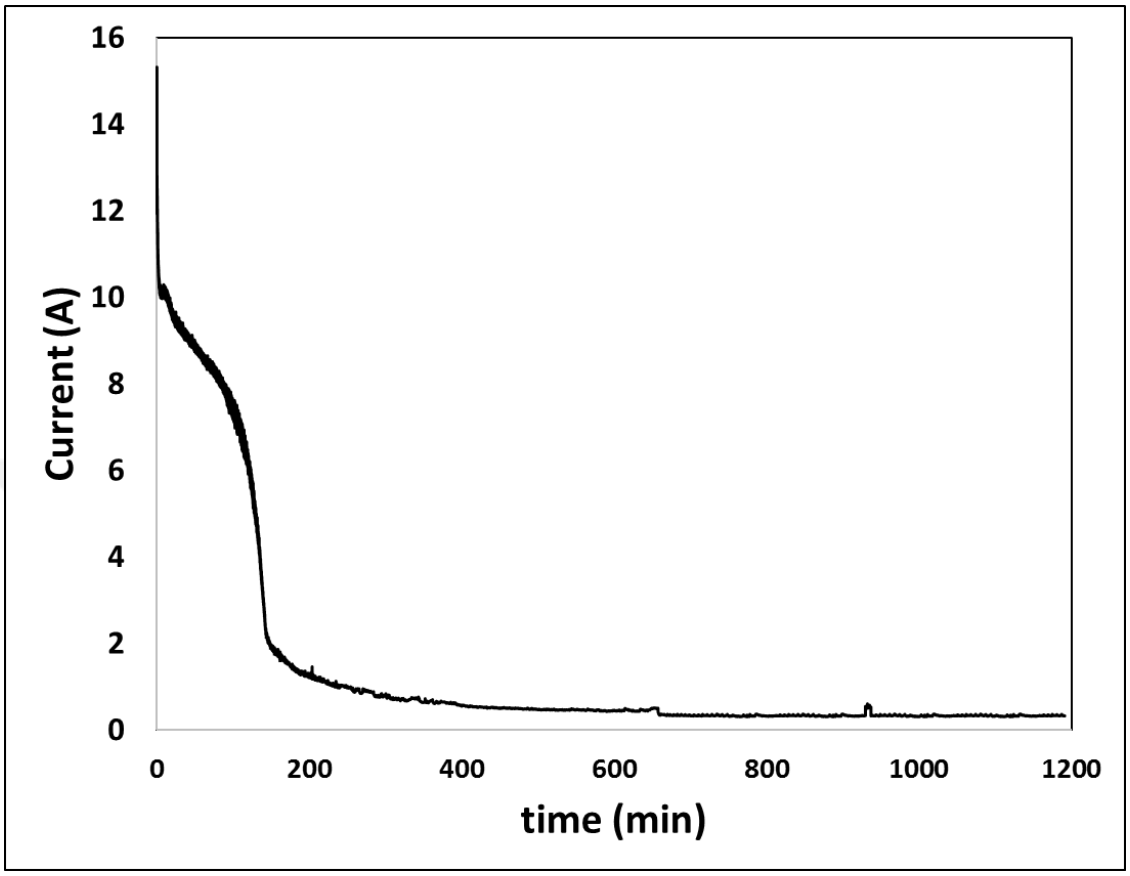


Figure 4.16 Chronoamperogram of the experiment conducted with 60 grams of $CaWO_4$

The photograph of the graphite rod (see Figure 4.17) after electrolysis demonstrated the abrasion present specifically at around the contact zone of graphite with the electrolyte. The first modification to overcome short circuit problem was the application of boron nitride coating to the graphite electrode. The photograph of the "boron nitride applied" graphite after the electrolysis is demonstrated in Figure 4.18. As it can be seen, the application could not sustain the electrolysis, due to excessive abrasion on the electrode surface the electrode could not be used for further experiments.

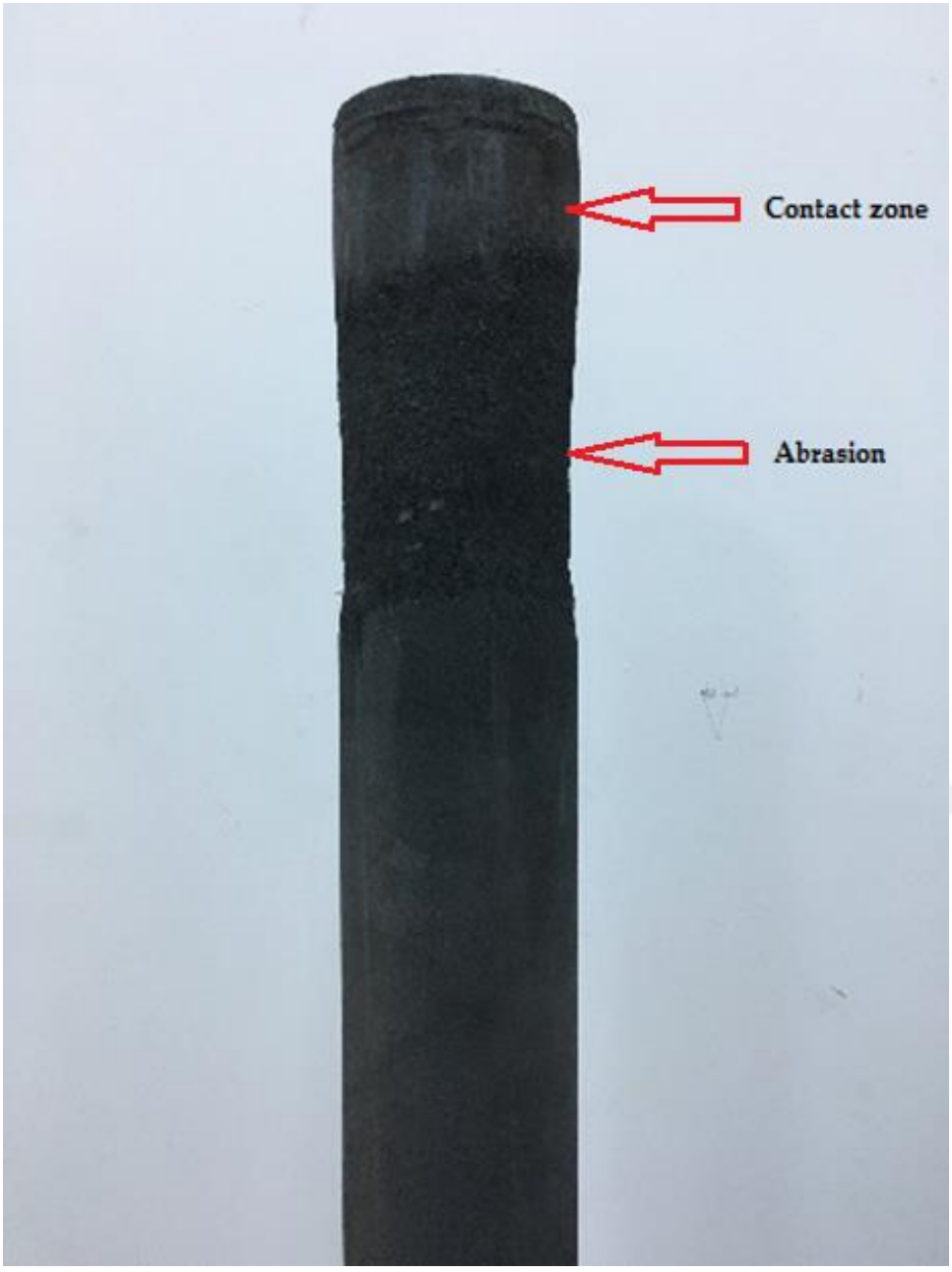


Figure 4.17 A photograph of the graphite electrode after electrolysis experiments



Figure 4.18 A photograph of the “boron nitride applied” graphite after the electrolysis

Another modification was to cover the non-contact zones of the graphite electrode with an alumina tube. The photograph of the alumina covered graphite after the electrolysis experiments is given in Figure 4.19. This modification provided considerable amount of reduction in the oxidation of graphite. The X-ray diffraction results of the samples produced after the modified system are given in Figure 4.20 and Figure 4.21. The modifications improved the amount of reduction of $CaWO_4$.



Figure 4.19 A photograph of the alumina coated graphite after the electrolysis experiments

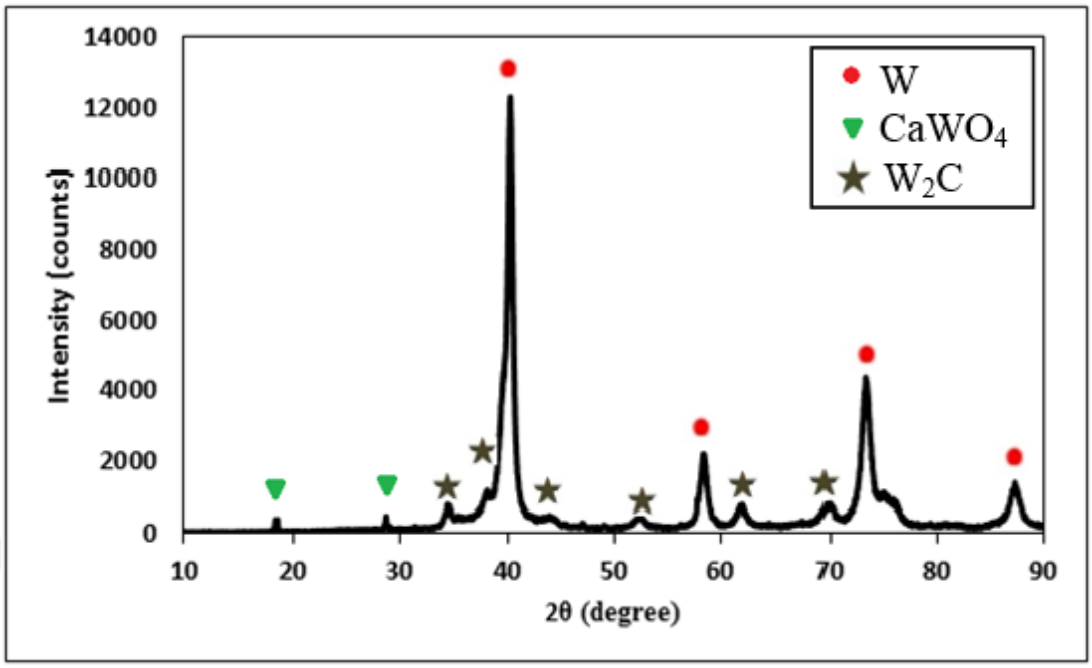


Figure 4.20 X-ray diffraction pattern of the one of the produced samples

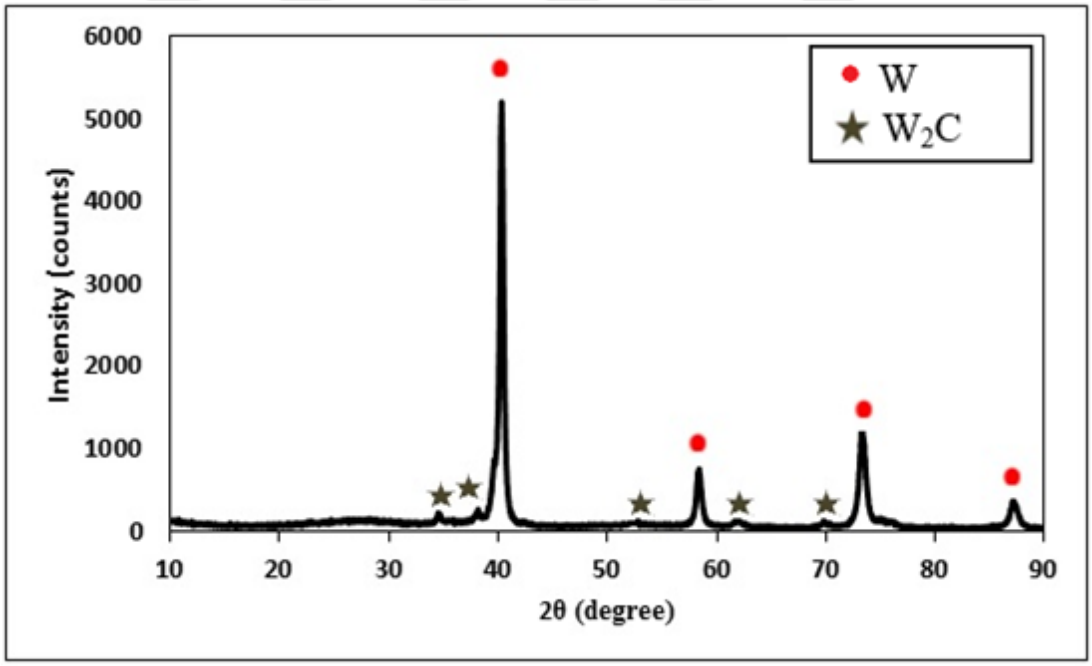


Figure 4.21 X-ray diffraction pattern of the one of the produced samples

As can be seen from the Figure 4.20 and Figure 4.21, tungsten production was succeeded with higher amounts than the previous experiments. However, the yield was not as high as the laboratory experiments. In addition, tungsten carbide formation was detected unlike the ones in the laboratory experiments. The presence of carbides of tungsten could be explained by the incorporation of carbon to the system via graphite electrode.

The SEM photograph of the produced powder is given in Figure 4.22. The agglomeration created a difficulty in particle size analysis. This sample was obtained from the reduced powder after the cleaning processes to prepare sample for further studies and to test sintering performance of the produced tungsten.

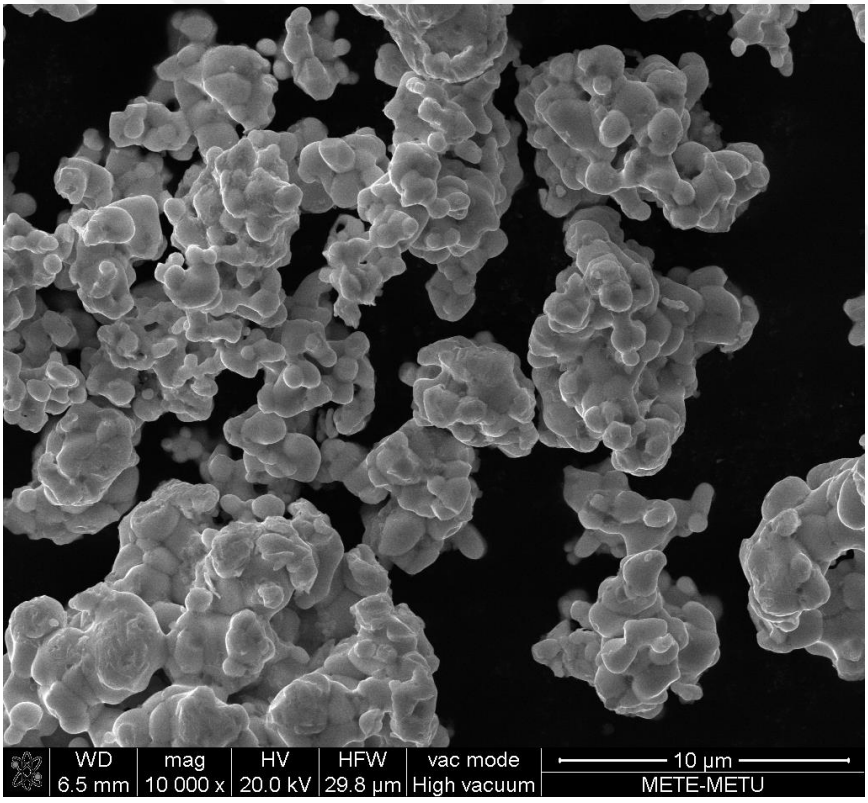


Figure 4.22 SEM photograph of the produced tungsten

CHAPTER 5

CONCLUSIONS

Production of tungsten refractory metal powders via electrochemical reduction of $CaWO_4$ in molten $CaCl_2$-NaCl salt mixture at 600^oC was investigated. The pulse current application was implemented for the electrochemical production of tungsten refractory metal powders for the first time. The pulse current experiments were performed by applying 0.1, 0.2, and 0.3 A average currents. Applied pulse duration was fixed at 1 ms while pulse relaxation durations were varied as 1, 4, 9 and 19 ms.

Pulse current reduction of $CaWO_4$ was successfully achieved. X-ray diffraction results of the samples indicated that they contained tungsten together with the calcium compounds which were the byproducts of the electrolysis. Subjection of the samples to dilute HCl solutions was successful to eliminate calcium compounds and isolate tungsten.

The energy consumption of the pulse current experiments was calculated by taking the actual amount of tungsten produced into consideration. The energy consumption of the pulse current experiments was in between 2.0 and 2.9 kWh per kg of tungsten. These values were lower than the studies for electrochemical reduction of $CaWO_4$ [34, 53] performed using constant voltage application.

The voltage values of the experiments were compared with the constant current experiments. Pulse current experiments provided lower voltage values than constant current experiments at the steady state conditions.

The SEM photographs of the samples demonstrated that the particle size of the produced powder was in nano-scale. The shapes of the particles were spherical in most of the experiments. However, the particles were in combination of the lath and spherical shapes in the samples produced with 0.2 A average current and 4-9 ms pulse relaxation time. The formation of these lath shaped particles mostly observed in the samples produced with 1 ms pulse relaxation time.

A larger scale tungsten production assembly was designed with a production capacity of 300 g tungsten per day. Tungsten production experiments were conducted by applying 2.8 to 3 V potential to system holding 60 to 100 grams of $CaWO_4$ as cathode material. The partial reductions on the preliminary experiments impelled the modifications on the system. The modifications in the cell and electrodes improved the amount of reduction of the raw material.

5.1 Recommendations for the Future Work

Pulse current experiments were promising in terms of the modification of the rate-limiting step of the electro-deoxidation which likely the diffusion of oxygen in the metal oxide at the cathode. Hence, the model that consists pulse and direct current or pulse and direct voltage reduction should be taken into practice for electro-deoxidation.

The effects of pulse parameters on the particle shape and size of the end product should be investigated.

Larger scale production of tungsten refractory metal powders should be investigated by employing pulse or pulse/reverse current/voltage.

REFERENCES

[1] British Geological Survey, "Risk List 2015 - An update to the supply risk index for elements or element groups that are of economic value," 2015. [Online]. Available: http://www.bgs.ac.uk/mineralsuk/statistics/risklist.html. [Accessed: 17-Oct-2016].

[2] K. S. Mohandas and D. J. Fray, "FFC Cambridge process and removal of oxygen from metal-oxygen systems by molten salt electrolysis: An overview," *Trans. Indian Inst. Met.*, vol. 57, no. 6, pp. 579–592, 2004.

[3] M. Erdogan and I. Karakaya, "Electrochemical reduction of tungsten compounds to produce tungsten powder," *Metall. Mater. Trans. B Process Metall. Mater. Process. Sci.*, vol. 41, no. 4, pp. 798–804, 2010.

[4] İ. Karakaya and M. Erdoğan, "Tungsten İçeren Bileşiklerden Elektrokimyasal Metotlarla Tungsten ve Tungsten Alaşımları Kazanımı", Turkish Patent Institute, TR 2007 07197 B, 2007.

[5] İ. Karakaya and M. Erdoğan, "Production of Tungsten and Tungsten Alloys from Tungsten Bearing Compounds by Electrochemical Methods,"Russian Agency for Patents and Trademarks, RU 2463387 C2,2012.

[6] İ. Karakaya and M. Erdoğan, "Production of tungsten and tungsten alloys from tungsten bearing compounds by electrochemical methods," WPO-WCT, WO 2009054819 A1, 2008.

[7] İ. Karakaya and M. Erdoğan, "Production of Tungsten and Tungsten Alloys from Tungsten Bearing Compounds by Electrochemical Methods," Canadian Intellectual Property Office, CA 2703400 A1, 2012.

[8] "International Tungsten Industry Association (ITIA)," 2011. [Online]. Available: http://www.itia.info/tungsten-properties.html. [Accessed: 05-May-2016].

[9] E. Lassner, S. Wolf-Dieter, E. Lüderitz, and H. U. Wolf, “Tungsten, Tungsten Alloys, and Tungsten Compounds,” *Ullmanns Encycl. Ind. Chem.*, vol. 37, pp. 119–126, 2012.

[10] R. H. Limbaugh, “Strategic Metals and National Defense: Tungsten in World War II (and Beyond) Tungsten in Peace and War,” *2006 Min. Hist. J.*, pp. 38–46, 2006.

[11] “Handbook for MTCR Guidelines and Annex.” 2014.[Online]. Available: https://fas.org/nuke/control/mtcr/text/mtcr_handbook_guide-annex.pdf

[12] “The Wassenaar Arrangement on Export Controls for Conventional Arms and Dual-Use Goods and Technologies,” 2016. [Online]. Available: http://www.wassenaar.org/control-lists/. [Accessed: 10-Dec-2016].

[13] S. M. Kimball, “Mineral Commodity Summaries 2016,” *U.S. Geol. Surv. Reston, Virginia 2016*, pp. 180–182.

[14] “Price book.” 2016. [Online]. Available: https://www.metalbulletin.com. [Accessed: 10-Dec-2016].

[15] P. Pitfield and T. Brown, “Tungsten - Commodity Profile,” [Online]. 2011. Available: www.bgs.ac.uk/DOWNLOADS/start.cfm?id=1981. [Accessed: 1-Dec-2015].

[16] H. L. Slatin, “Electrolytic Production of Tungsten and Molybdenum,” United States Patent Office, US 3297554, 1966.

[17] M. Erdoğan, “Recovery of Tungsten from Tungsten Bearing Compounds” Middle East Technical University,Department of Metallurgical and Materials Engineering Ankara, Turkey, 2013.

[18] T. P. Hoar and R. G. Ward, “The electrolytic removal of oxygen, sulphur, selenium, and tellurium from molten copper,” *J Inst Met*, vol. 90, pp. 6–12, 1962.

[19] T. H. Okabe, T. Oishi, and K. Ono, “Deoxidation of titanium aluminide by Ca-Al alloy under controlled aluminum activity,” *Metall. Trans. B*, vol. 23, no. 5, pp. 583–590, 1992.

[20] T. H. Okabe, R. O. Suzuki, T. Oishi, and K. Ono, “Production of Extra Low Oxygen Titanium by Calcium--Halide Flux Deoxidation,” *Tetsu-to-Hagane(Journal Iron Steel Inst. Japan)*, vol. 77, no. 1, pp. 93–99, 1991.

[21] K. Ono, T. Okabe, M. Ogawa, and R. Suzuki, “Production of Titanium Powders by the Calciothermic Reduction of TiO sub 2,” *Tetsu-to-Hagane(J. Iron Steel Inst. Jpn.)*, vol. 76, no. 4, pp. 568–575, 1990.

[22] G. Z. Chen, D. J. Fray, and T. W. Farthing, “Direct electrochemical reduction of titanium dioxide to titanium in molten calcium chloride,” *Nature*, vol. 407, no. 6802, 2000.

[23] E. Gordo, G. Z. Chen, and D. J. Fray, “Toward optimisation of electrolytic reduction of solid chromium oxide to chromium powder in molten chloride salts,” *Electrochim. Acta*, vol. 49, no. 13, pp. 2195–2208, 2004.

[24] X. Jin, P. Gao, D. Wang, X. Hu, and G. Z. Chen, “Electrochemical preparation of silicon and its alloys from solid oxides in molten calcium chloride.” *Angew. Chem.*, vol. 116, pp. 751–754, 2004.

[25] W.K. Han, J.W. Choi, G.H. Hwang, S.J. Hong, J.S. Lee, and S.G. Kang: Appl. “Fabrication of Cu Nano Particles by Direct Electrochemical Reduction from CuO Nano Particles” *Surf. Sci., 2006*, vol. 252, pp. 2832–38.

[26] G.Z. Chen and D.J. Fray, "Novel direct electrochemical reduction of solid metal oxides to metals using molten calcium chloride as an electrolyte" *Progress in Molten Salt Chemistry 1*, 2000, pp. 157–62.

[27] G.Z. Chen and D.J. Fray, "Electro-deoxidation of Metal Oxides", Light Metals, TMS, New York, NY, 2001, pp. 1147–52.”

[28] A. M. Abdelkader, A. Daher, R. A. Abdelkareem, and E. El-Kashif,

"Preparation of zirconium metal by the electrochemical reduction of zirconium oxide," *Metall. Mater. Trans. B Process Metall. Mater. Process. Sci.*, vol. 38, no. 1, pp. 35–44, 2007.

[29] K. Dring, R. Bhagat, M. Jackson, R. Dashwood, and D. Inman, "Direct electrochemical production of Ti–10W alloys from mixed oxide preform precursors," *J. Alloys Compd.*, vol. 419, no. 1, pp. 103–109, 2006.

[30] R. Bhagat, M. G. Jackson, D. Inman, and R. J. Dashwood, "Production of Ti-W alloys from mixed oxide precursors via the FFC Cambridge process," *J. Electrochem. Soc.*, vol. 156, no. 1, p. E1, 2009.

[31] A. Packter and B. N. Roy, "The crystallisation of alkaline-earth metal tungstates (molybdates, chromates, and sulphates) from metal chloride melts," *Krist. und Tech.*, vol. 6, no. 1, pp. 39–51, 1971.

[32] M. Erdoğan and İ. Karakaya, "On the Electrochemical Reduction Mechanism of $CaWO_4$ to W Powder," *Metall. Mater. Trans. B*, vol. 43, no. 4, pp. 667–670, 2012.

[33] D. Tang, W. Xiao, H. Yin, L. Tian, and D. Wang, "Production of Fine Tungsten Powder by Electrolytic Reduction of Solid $CaWO_4$ in Molten Salt," *J. Electrochem. Soc.*, vol. 159, no. 6, p. E139, 2012.

[34] D.-H. Tran-Nguyen, D. Jewell, and D. J. Fray, "Electrochemical preparation of tungsten, tungsten carbide and cemented tungsten carbide," *Trans. Institutions Min. Metall. Sect. C Miner. Process. Extr. Metall.*, vol. 123, no. 1, pp. 53–60, 2014.

[35] E. Ergül, "Reduction of Silicon Dioxide by Electrochemical Deoxidation," Middle East Technical University,Department of Metallurgical and Materials Engineering Ankara, Turkey, 2010.

[36] Y. Ueda, N. Hataya, and H. Zaman, "Magnetoresistance effect of Co/Cu multilayer film produced by electrodeposition method," *J. Magn. Magn.*

Mater., vol. 156, no. 1, pp. 350–352, 1996.

[37] M. S. Chandrasekar and M. Pushpavanam, "Pulse and pulse reverse plating-Conceptual, advantages and applications" *Electrochim. Acta*, vol. 53, no. 8, pp. 3313–3322, 2008.

[38] S. Kainuma, S. Ishikura, K. Hisatake, "Dependence on GMR on copper layer thickness in electrodeposited CoNiCu/Cu multilayer", *J. Magn. Soc. Jpn.* 21, 1995, p. 889.

[39] T. Houga, A. Yamada, Y. Ueda, "Electric Properties of Ni-Co Based Multilayer Films Produced by Pulse Control Electrodeposition Method" *J. Jpn. Inst. Met. 64* , 2000, p.739.

[40] M. Alper, K. Attenborough, R. Hart, S.J. Lance, D.S. Lashmore, C. Younes,W. Schwarzacher,"Giant magnetoresistance in electrodeposited superlattices" *Appl. Phys. Lett.* vol. 63, 1993, p. 2144.

[41] M. Paunovic, M. Schlesinger, Fundamenthals of Electrochemical Deposition, Electrochem. Soc.. John Wiley and Sons, New York, 1998

[42] A.M. El-Sherik, U. Erb, J. Page, "Microstructural evolution in pulse plated nickel electrodeposits" *Surf. Coat. Technol.* vol.88, p.70, 1996

[43] S. Roy, A. Connell, M. Ludwig, N.Wang, T.O. Donnell, M. Brunet, P.M. Closkey, C.O. Mathuna, A. Barman, R.J. Hicken, "Pulse reverse plating for integrated magnetics on Si" *J. Magn. Magn. Mater. pp* 290–291, vol 1524, 2005

[44] "Collection of Phase Diagrams" no date. [Online]. Available: http://www.crct.polymtl.ca/fact/pdweb.php. Accessed: [12-Sep-2015]

[45] İ. Karakaya, "Electrochemical Determination of Thermodynamic Properties of Magnesium Cell Electrolyte the System $MgCl_2$-NaCl-$CaCl_2$", Department of Mining and Metallurgical Engineering, McGill University, Montreal, Canada, 1985

[46] X. Chang, S. Sun, L. Dong, Y. Dong, and Y. Yin, “Large-scale production of tungsten trioxide nanoparticles for electrochromic application,” *RSC Adv.*, vol. 4, no. 18, p. 8994, 2014.

[47] O. G. Göksu, M. Erdoğan, and İ. Karakaya, “A Pulse Voltage Application in Electrochemical Reduction of Solid $CaWO_4$ Powder” *ECS Transactions*, vol. 72, no. 33, pp. 31–39, 2016.

[48] A. Gomes and M. I. Da Silva Pereira, “Pulsed electrodeposition of Zn in the presence of surfactants,” *Electrochim. Acta*, vol. 51, no. 7, pp. 1342–1350, 2006.

[49] Z. Feng, E. Granda, and W. Hung, “Experimental Investigation of Vibration-Assisted Pulsed Electrochemical Machining 2 Literature Review,” *Procedia Manuf.*, pp. 1–17, 2016.

[50] M. Erdoğan, “Tungsten Production by Electrodeoxidation”, Middle East Technical University,Department of Metallurgical and Materials Engineering Ankara, Turkey, 2007.

[51] Pistorius, P.C. and D.J. Fray, “Formation of silicon by electrodeoxidation, and implications for titanium metal production.” *Journal of the South African Institute of Mining and Metallurgy*, vol 106, pp. 31 - 41, 2006

[52] W. Xu and L. Chunfa, “Preparation and characterization of tungsten powder through molten salt electrolysis in a $CaWO_4$-$CaCl_2$-NaCl system,” *Int. J. Refract. Met. Hard Mater.*, vol. 31, pp. 205–209, 2012.

[53] Primary Aluminum Smelting Power Consumption (2016). [Online]. Available: http://www.world-aluminium.org/statistics/primary-aluminium-smelting-power-consumption/ [Accessed: 17-Oct-2016].

[54] W. Wulandari, G. A. Brooks, M. a Rhamdhani, and B. J. Monaghan, “Magnesium : Current and Alternative Production Routes,” *Chemeca 2010 Eng. Edge.*, p. 347, 2008.